

Studies on the regulation of gene
expression by a 0.3-kb fragment
containing the R-U5-5' leader sequence of
murine leukemia virus

September, 2013

Choo Yeng Cheng

INTRODUCTION

I. An Overview of the Legacy and Shift in Retroviral Studies	1
II. General Properties of Retroviruses	4
III. Murine Retroviruses and disease	5
IV. The neuropathogenic determinant of Friend-MLV clone A8 and its relation to the present study	8

**CHAPTER 1: Kinetic Studies of the effects of the 0.3-kb fragment
on viral gene expression and viral production****Materials and Methods**

• Viruses and cells	12
• Time course analysis of viral proliferation	12
• Focal Immunoassay	12
• Immunoblot analysis	13
• RNA extraction and quantification	13
• Genomic DNA extraction and quantification	14

Results	15
----------------	----

Discussion	23
-------------------	----

**CHAPTER 2: Mechanism by which the 0.3-kb fragment participates
in protein expression****Materials and Methods**

• Vector construction	26
• Cell culture	27
• Transfection and assay for luciferase activity	28
• RNA extraction and quantification	28
• Genomic DNA extraction and quantification	29
• Cell fractionation	29
• Determination of poly (A) tail length	29

Results	
• The 0.3-kb fragment effects on the luciferase protein expression	31
• The 0.3-kb fragment did not affect the poly (A) tail length of mRNA or the nuclear-cytoplasmic distribution of <i>luc</i> -mRNA	34
• Point mutation analysis	38
• Secondary structure analysis	40
• Alignment of the 0.3-kb fragment sequences among gammaretroviruses	42
Discussion	45
CONCLUSION	49
REFERENCES	51
ACKNOWLEDGEMENTS	60
Figures and Tables	
Fig. 1-1 Alignment of the 0.3-kb KpnI and AatII fragment	16
Fig. 1-2 Structures of the R7f and Rec5 viruses	17
Fig. 1-3 Viral titers in cultured supernatants of cells infected with R7f or Recc5	18
Fig. 1-4 Expression of Env and Gag Protein in NIH3T3 cells infected with R7f or Rec5	19
Fig. 1-5 Relative amounts of total viral mRNA and spliced <i>env</i> -mRNA	21
Table 1-1 Comparison of viral protein expression levels, <i>env</i> -mRNA and total viral mRNA levels, and the ratios of the amount of <i>env</i> -mRNA to that of total viral mRNA	22
Fig. 2-1 Structures of luciferase expression vectors	32
Fig. 2-2 Relative Luciferase activity and relative amount of total mRNA and spliced mRNA	33
Fig. 2-3 Determination of poly (A) tail length	35
Fig. 2-4 Nuclear-cytoplasmic distribution of <i>luc</i> -mRNA	37
Fig. 2-5 Luciferase activity of mutation series vectors	39
Fig. 2-6 Predicted secondary structure of the 0.3-kb fragment of A8 and 57 sequence	41
Table 2-1 Alignment of the 0.3-kb fragment sequence of the gamma retroviruses	43

INTRODUCTION

I. An Overview of the Legacy and Shift in Retroviral Studies

The beginning of retrovirus studies has much to do with finding the cause for cancer. The story of how three scientists, Vilhelm Ellerman and Oluf Bang in 1908 and Peyton Rous in 1911 were able to show the transmissibility of cancer in chicken through inoculating cell-free tumour extract is now famously being told and quoted as the beginning of the discovery of retroviruses (Ellerman and Bang, 1908; Peyton., 1911). After the observations in avians, the first mammalian tumor causing agent was isolated in 1936, where Bittner was able to show that breast cancer was transmissible through the milk of the nursing mouse mothers which had a very high incidence of breast cancer (Bittner, 1942). Subsequently, more diseases are described to be correlated with the existence of retroviruses in a variety of animals including mouse (Gardner, 1978), felines (Hardy, 1982), caprines (Cork et al., 1974; Crawford et al., 1980) and humans (Uchiyama T, 1977).

Early retrovirus studies have largely involved microscopy analysis and classifications of many classes of retroviruses based on its morphology and cell tropism (Coffin et al., 1997b). This period can be known as the classic era where retroviruses are studied as a discrete and vigilant entity from the living host cell. However, with the advent of molecular biology techniques that allows large scale examination of proteins, RNA and DNA of retroviruses and cell properties, the view of retrovirus has taken change expansively in this new era and we are perplexed with one question.

Just what are the traits unique to a retrovirus? Astoundingly, unlike the classic era where retrovirus is thought to possess distinctive characteristics, in the present era, retrovirus is practically undistinguishable from a living cell in multi-ways. Reverse transcriptase activity that was once thought to be the defining hallmark of retrovirus characteristic (Baltimore, 1970; Coffin et al.,

1997d; Temin and Mizutani, 1970) is no longer exclusive to a retrovirus. Reverse transcriptase activity is now known to be inherently important for various cell physiological activities such as embryonic cell proliferation, differentiation and tumor progression (Sinibaldi-Vallebona et al., 2006; Spadafora, 2004, 2008). Besides, it is also becoming more apparent that what contained within the matured virion is much more than just viral genomic RNA and viral proteins. Retroviruses are known to also package cellular RNAs and proteins and the enrichment of these cellular products suggests that there is a selective mechanism for incorporation which functions remains to be elucidated (Houzet et al., 2007; Muriaux and Rein, 2003; Onafuwa-Nuga et al., 2006; Segura et al., 2008).

The most bewildering of all is perhaps the association of retrovirus with the newly emerging field of membrane excreted vesicles for intercellular communications, the exosomes (Mittelbrunn and Sanchez-Madrid, 2012; Vlassov et al., 2012). Retroviruses and exosomes are so identical that it first led to the problems of isolating and purification of these two vesicles (Bess et al., 1997; Gluschankof et al., 1997). The inability to carefully sort out between the two will have major implications that lead to fundamental questions as to how to derive meaningful interpretations on experiments done on retroviral studies? Notably, the most seemingly convincing purification method were developed a decade later by immune-depleting the exosomes marker acetylcholinesterase (AChE) to obtain highly purified HIV-1 and highly purified exosome preparations (Cantin et al., 2008). As interests begin to grow in the field of exosomes (Thery, 2011) that was previously thought to be merely cellular debris, unexpectedly, researches continue to observe striking similarities between the two whether in vesicle biogenesis, membrane composition, mediation by antigen presenting cells in migration within the body, and mode of activating humoral responses (Cantin et al., 2008; Izquierdo-Useros et al., 2009; Narayanan et al., 2013; Nguyen et al., 2003; van Kooyk and Geijtenbeek, 2003). These observations supported by empirical data have led some researchers to introduce Trojan exosome hypotheses which state that the retroviruses have

adopted the non-viral exosome exchange pathway for the formation of infectious retroviral particles and Env-independent mode of infection (Gould et al., 2003; Izquierdo-Useros et al., 2010).

The enduring list of indiscriminating features between retroviruses and living cells seems to be dominating many if not most of the discoveries in the 21st century. Another discovery to attest to this paradigm shift is the discovery of endogenous retrovirus (ERVs) in a variety of animals (Herniou et al., 1998; Weiss, 1996) in addition to the findings that 8% of our genome is derived from sequences with similarity to infectious retroviruses (Bannert and Kurth, 2004; Griffiths, 2001; Li et al., 2001). Finding that our mammalian genome is represented by a significant proportion of retroviral remnants had caused a critical question of whether retroviruses have always been an invader to its host or did retroviruses originate from their host cells? While the quest to understand the importance of the retroviral sequences in mammalian genome still has a long way to go, consensually, we now understand that merely grouping living things into what is “host or cellular” versus what is “viral” appears facade and an oversimplified view which would disengage us from grasping a complete view of what natural science studies have to offer. Study of retrovirus is just one of the kinds of instrument that is going to blur the definition between host and pathogens, health and diseases. Therefore, by taking note of the resemblance and close existence between retrovirus and host cell calls for the design of un-prototypical treatment that may help drive the success of relieving AIDS-inclining patients.

Lastly, in discussing about the interests in the field of retroviruses, one can definitely not be able to ignore the development of the use of retrovirus gene in therapeutic gene therapy. Technically, gene therapy refers to the transfer of a gene that encodes a functional protein into a cell or the transfer of an entity that will alter the endogenous gene in a cell (Kresina, 2002). The choice of using retrovirus as the “vehicle” for facilitating the transfer of genetic material into the cell derives from the defining hallmark of retrovirus sequences ability to reverse transcribe its genome from RNA into DNA and further incorporating its own DNA into the host’s genome, thereby

establishing itself permanently as part of the host genome. Experimentally, retroviral vectors have been used extensively in animals and it has also been used majorly for ex vivo gene therapy (Durand et al., 2012; Kay, 2011; Suerth et al., 2012a; Suerth et al., 2012b). Needless to say, just the idea of introducing a gene extraneously and using retroviruses as the basis for the vector will immediately prompt anybody to think about the risks that it presents (Kappes and Wu, 2001; Wilson and Cichutek, 2009). The future of scientific endeavours however is such that it will continuously present us with more pressing issues such as knowing between the boundaries of scientific pursuits that will not turn into disastrous events and advancing knowledge about life and biology for medical purposes. Retroviruses, once again stand at the crossroad of this scientific feat.

II. General Properties of Retroviruses

The genome of retroviruses is composed of two copies of positive single-stranded RNA genome of 7 to 10kb (Coffin et al., 1997c). Based on electron microscope morphology of virions and analysis of genome sequences, retroviruses have been grouped into three subfamilies, oncoviruses, lentiviruses and spumaviruses. However, based on comparison with the reverse transcriptase (RT) gene, a more adaptable classification has been established and seven genera have been introduced to classify retroviruses: alpharetrovirus, betaretrovirus, gammaretrovirus, deltaretrovirus, epsilonretrovirus, lentivirus and spumavirus (Gifford et al., 2005; King et al., 2012; Xiong and Eickbush, 1990). These seven genera can be broadly classified into two categories. Alpha-, beta-, gamma- are genetically simple while delta-, epsilon-, lenti- and spuma- are considered complex. A simple retrovirus is characterized by having only the *gag*, *pol* and *env* genes, while complex retroviruses contain extra genes, which products have regulatory or accessory functions, in addition to the *gag*, *pol* and *env* genes.

The simple retroviruses, including murine leukemia virus (MLV), are characterized by a

coding structure in which the *gag*, *pol* and *env* genes are flanked by two long terminal repeats (LTRs), a 5'LTR and 3'LTR. Proteins responsible for the constitution of the inner structures of the virion are encoded by the *gag* gene, which includes the matrix, capsid and nucleocapsid proteins. The *pol* gene encodes the enzymatic proteins, i.e. the reverse transcriptase, protease, integrase and RNase H and the *env* gene encodes the proteins protruding out from the viral particle surface, namely the surface (SU) and transmembrane (TM) proteins (Coffin et al., 1997c).

Transcription begins from the R region of the 5'LTR and ends at the polyadenylation signal located at the R region at the other end of the 3'LTR. A 5'splice site (5'ss) is located in the 5'leader sequence and a 3'splice site (3'ss) is located at the 3' end of the *pol* gene. Only a singly spliced mRNA is usually found in simple retroviruses. Gag and Pol proteins are translated from the unspliced full-length viral mRNA, and the Env protein is translated from the spliced *env*-mRNA (Coffin et al., 1997c). In contrast, it is reported that HIV-1 could generate up to 40 different spliced RNAs using four 5'ss and nine 3'ss (Delgado et al., 2012; Seelamgari et al., 2004) in a complex retrovirus. In recent years however, it has been reported that simple retroviruses harbor more used alternative splice sites (Déjardin et al., 2000) than previously known. The functions of these alternatively spliced variant remains to be elucidated but one of it, the SD' RNA which utilizes a 5'ss within the capsid-coding region to the canonical envelope 3'ss has been reported that its incorporation into the virion is required for optimal viral infectivity (Maurel et al., 2007).

III. Murine Retroviruses and disease

Most of the names used to coin MLVs are the reflection of the direct observations of the malignancies caused by the retrovirus after inoculation into laboratory strain mice during the time of the retrovirus discoveries. With the “cell-transforming” ability of retroviruses, among the malignancies observed includes rapid sarcoma by Harvey sarcoma virus (Ha-MSV) (Harvey, 1964),

Kirsten murine sarcoma (Ki-MSV) (Kirsten and Mayer, 1967); FBR osteosarcoma virus, lymphosarcoma caused by Abelson Murine Leukemia Virus (Ab-MLV) (Abelson and Rabstein, 1970a, b); splenomegaly by Friend spleen focus-forming virus (F-SFFV) (Troxler et al., 1977a; Troxler et al., 1977b); and hematological abnormalities by F-MLV (Friend, 1957), Moloney MLV (Mo-MLV) (Moloney, 1960), and Rauscher-MLV (Rauscher, 1962). Subsequently, neurological disorders and immunodeficiencies were also observed in the infected host, which is apparent through complications such as complete or hindlimb paralysis, ataxia and tremor (Gomez-Lucia, 2005; Nagra et al., 1992). While the route of how MLVs cause diseases is still beyond complete comprehension, studies of MLVs has provided the models for diseases caused by retrovirus infection in explaining neoplasm transformation and encephalopathies. The standard models of how malignancies and encephalopathies advance, both caused by MLVs, are distinct from each other.

In explaining about malignancies or the oncogenic potential of retroviruses, has led to the naming of various oncogenic genes in cells known as proto-oncogenes. The proto-oncogene is thought to be incorporated into the genome of the infecting MLVs through recombination processes. As a result of this recombination, the retrovirus will possess a high transforming ability, however with the loss of its replicative ability and the retrovirus is known to be replication “defective”. The high transforming ability of the replication defective retrovirus is the result of co-operation with a “helper” retrovirus that will provide the necessary genes and proteins that help the defective retrovirus to induce host cell and replicate. Various proto-oncogenes that are incorporated into retrovirus has been discovered to date (Maeda et al., 2008; Vogt, 2012) which includes growth factors (V-sis); growth factor receptors (v-erbB); intracellular tyrosine kinases (v-src, v-fps, v-fes, v-abl); members of the G protein family (H-ras, Ki-ras); and transcription factors (v-myc, v-erbA) . The altered expression rates of the oncogenes are responsible for the tumorigenesis. Alternatively, the transforming ability of retrovirus is explained through direct integration of the viral genome in the vicinity of the regulatory genes which results in activation or silencing of the genes (Coffin et al.,

1997a; Vogt, 2012). How the incorporation of a proto-oncogene into the retrovirus genome or integration of provirus into the host genome could be associated with such deadly consequences in the host is unclear, but for the full transformation of the tissue, a cascade of proteins may have to be activated or its expression altered. Similarly, for the transformation via provirus integration, different regions of the host DNA may have to be integrated and infection is likely to take place several times (Bishop, 1991; Dudley et al., 2002; Kung et al., 1991).

While the effect of malignancies is caused almost actively by the retrovirus ability to integrate and replicate in target tissues, the effect towards neurological disorders are less direct. Indirect mechanism of retrovirus in leading to neuropathogenicity includes observations that severity or occurrence of clinical disease is not correlated with the virus expression or viral titer in CNS parenchyma (Takase-Yoden and Watanabe, 1997). Microglia is mainly the infected cells in CNS cell population and sometimes, astrocytes or oligodendrocytes, while neurons are rarely and almost never infected (Gomez-Lucia, 2005). Mice are also only susceptible when retrovirus is inoculated in newborn mice as no spongiform of neuron cells or clinical disease is observed when experiments are done with prenatal and postnatal day 6 mice (P6) (Brooks et al., 1981; Czub et al., 1991).

As immediate consequences derived from retrovirus replication in neuron cells could not be seen, expression of cellular and viral proteins is bring forth to explain the toxicity towards neuron cells. Production of cellular effectors, such as cytokines by astrocytes, endothelial and microglia has been proposed to injure neurons (Askovic et al., 2001; Bonwetsch et al., 1999; Choe et al., 1998; Miller and Meucci, 1999; Nagra et al., 1994; Peterson et al., 2001). Neurotoxicity is also induced by oxidative stress (Jinno-Oue et al., 2003; Jolicoeur et al., 2003; Zachary et al., 1997). Binding of Env proteins to mCAT-1 (a basic amino acid transporter which serves as the receptor for ecotropic MLVs) has been proposed to mediate the induction of oxidative injury to neuron cells. Through deprivation of arginine as the precursor block for nitric oxide (NO), homeostasis of NO is

disrupted (Lynch et al., 1996) which leads to toxicity towards neurons and increase permeability of the blood-brain barrier (Wilt et al., 2000).

The involvement of viral Env in inducing neuropathogenicity has been highly regarded and demonstrated in multiple studies (DesGroseillers et al., 1984; Masuda et al., 1993; Masuda et al., 1992; Paquette et al., 1989; Szurek et al., 1988; Takase-Yoden and Watanabe, 1997; Yuen et al., 1986). For example, stress is induced at the ER level produced by the inefficient processing or folding of neuropathogenic Env protein (Dimcheff et al., 2003; Dimcheff et al., 2004; Kim et al., 2004; Portis et al., 2009; Qiang et al., 2004; Qiang et al., 2006; Szurek et al., 1990a; Szurek et al., 1990b). Notably, two isoforms of mature SU protein can be derived namely the gp65 and gp70 variants. Since gp65 is the isoform observed to be incorporated into virions, it has been proposed that neurotoxicity may emerge from the gp70. Furthermore, an association between the cellular localization of the Env proteins has been documented (Portis et al., 1990). The authors reported that when the effect of spongiform induction was most evident, the Env proteins accumulated in the distal axons in the cerebellar cortex neurons, instead of in the neural bodies (Askovic et al., 2001).

IV. The neuropathogenic determinant of Friend-MLV clone A8 and its relation to the present study

In a previous study of the viral clone A8, we showed that a high level of expression of A8-Env protein in rat brain was correlated with neuropathogenicity (Takase-Yoden et al., 2006; Takase-Yoden and Watanabe, 2005; Watanabe and Takase-Yoden, 2006). Studies with chimeras constructed from the A8 virus and the non-neuropathogenic Fr-MLV clone 57 identified a 0.3-kb KpnI-AatII fragment containing the R-U5-5' leader sequence as an important determinant of neuropathogenicity, in addition to the *env* gene of A8 as the primary determinant (Takase-Yoden and Watanabe, 2005). Chimeric virus Rec5, which contains the A8-*env* gene on the background of

57, did not exhibit neuropathogenicity. In contrast, the chimeric virus R7f, which contains a 0.3-kb fragment of A8 and the A8-*env* gene on the background of 57, induced spongiform neurodegeneration. It has been shown that the expression level of Env protein in both R7f-infected cultured cells and in brains of R7f-infected rats was higher than in the Rec5-infected cultured cells and brains of Rec5-infected rats (Takase-Yoden et al., 2006; Takase-Yoden and Watanabe, 2005). Comparison of the sequences between A8 and 57 revealed that they had 17 nucleotides difference (Fig. 1-1) and within this fragment contains functional domains, such as a signal for poly (A) addition to mRNA that works in the 3' long terminal repeat (LTR), a primer binding site (PBS) for reverse transcription, and a 5'ss. However the steps of gene expression at which the 0.3-kb fragment may influence Env expression have yet to be elucidated.

Given that the 0.3-kb fragment containing the R-U5-5'leader sequence is the first untranslated region that exists in all variants of retroviral transcripts, this region dynamically impacts various stages of the viral life cycle. The R region, present at both ends of viral RNA, mediates the jump of reverse transcriptase from the 5' site to the 3' site during the synthesis of minus-strand DNA (Berkhout et al., 2001; Gilboa et al., 1979), possibly by mediating genome circularization (Beerens and Kijems, 2010; Gee et al., 2006; Ooms et al., 2007). In addition, the stem-loop structure of the R region is important for transcriptional activity and enhances gene expression of a variety of retroviruses, including HIV, human T cell leukemia virus, bovine leukemia virus, avian reticuloendotheliosis virus, MLV, mouse mammary tumor virus, human foamy virus, and spleen necrosis virus (Bannwarth and Gatignol, 2005; Derse and Casey, 1986; Hauber and Cullen, 1988; Jones et al., 1988; Kiss-Toth and Unk, 1994; Montagne and Jalinot, 1995; Ohtani et al., 1987; Pierce et al., 1993; Ridgway et al., 1989; Trubetskoy et al., 1999). The end of the U5 region is marked by the beginning of the primer binding site (PBS) for reverse transcription (Aiyar et al., 1992; Lund et al., 1999; Morris and Leis, 1999). The surrounding region of U5 with the 5'leader sequence (which extends from the PBS to the AUG codon of *gag*) has specific

sequences with distinct secondary structure features (Berkhout and van Wamel, 2000; Mougel et al., 1993). There is strong evidence that this region is robust and that the secondary structures presented are fine-tuned to regulate one stage of RNA processes, and they could also act as inhibitors for other processes (Miller et al., 1997). For example, the stem loop of DIS-1, which plays a role in initiating viral RNA dimer formation, is situated immediately downstream of the 5'ss. By deleting this stem loop structure, the splicing efficiency of a modified Akv-MLV increased 5-10 fold, illustrating the modulating effect of DIS-1 on the production of viral genomes (Aagaard et al., 2004). Interestingly, sequences upstream of 5'ss have also been reported to be limiting factors for splicing regulation (Kraunus et al., 2006). A secondary structure known as the B monomer was presented in Mougel et al. (Mougel et al., 1993) and is a discerning trait in the MLV. This secondary structure, which is adopted in the dimeric RNA form, has also been shown to limit the recognition of U1snRNA to the splice donor, thereby also regulating the viral RNA production volume. Finally, the highly dynamic encapsidation structure that has been studied extensively in the prototype of MLV, Moloney MLV (Mo-MLV) (Basyuk et al., 2005; D'Souza et al., 2004; Miyazaki et al., 2010), is important for dimerization of the genomic RNA (Badorrek et al., 2006; Prats et al., 1990). It includes an IRES (internal ribosomal entry segment) (Berlioz and Darlix, 1995; Vagner et al., 1995) and also functions in the transport of viral intron-containing RNAs from the nucleus to the cytoplasm (Basyuk et al., 2005; Smagulova et al., 2005).

In Chapter 1, our goal was to apply kinetics analysis to study the effect of the 0.3-kb fragment on viral gene expression and viral production of two viruses namely R7f, carrying a 0.3-kb fragment of A8 and the A8-*env* gene on the background of the non-neuropathogenic Fr-MLV clone 57-and Rec5, carrying the A8-*env* gene on the background of 57. These analyses suggested that the 0.3-kb fragment influenced the expression level of the Env protein by regulating the amount of spliced-mRNA rather than the amount of total viral mRNA or viral production.

In Chapter 2, the role of the 0.3-kb fragment was further analyzed by utilizing luciferase

expression vectors. These luciferase expression vectors contain the full-length proviral genome of Fr-MLV with the *luciferase (luc)* gene incorporated in place of the *env* gene. The effects of the 0.3-kb fragment on several steps affecting protein expression levels in cells were examined. The results showed that the 0.3-kb fragment of A8 enhanced protein expression levels from the spliced mRNA through up-regulating the efficiency of splicing compared with the 0.3-kb fragment of 57, rather than through increased transcription, poly (A) addition to mRNA, or nuclear export of spliced mRNA. Furthermore, we investigated more specifically the roles of the 17 nucleotides that differ between A8 and 57 sequences in defining the function of the 0.3-kb fragment. Lastly, we discuss the possible mechanism by which the 0.3-kb fragment participates in protein expression.

CHAPTER 1

Kinetic Studies of the effects of the 0.3-kb fragment on viral gene expression and viral production

❖ **Materials and Methods**

- **Viruses and cells**

DNA clone of R7f and Rec5 was constructed as previously described (Takase-Yoden and Watanabe, 2005). The infectious DNA clone of R7f and Rec5 was transfected into NIH3T3 cells, and a virus-producing cell culture was established. The supernatants of these cells were used to infect M.dunni cells, and virus-producing cultures were used in the experiments. NIH3T3 cells were grown in Dulbecco's Modified Eagle Medium – low glucose (SIGMA). M.dunni cells were grown in RPMI1640. Both medium were supplemented with 10% fetal calf serum (MP Biomedicals) and penicillin (GIBCO) and cells were incubated at 37°C; 7% CO₂ atmosphere.

- **Time course analysis of viral proliferation**

NIH3T3 cells were seeded at 2×10^5 cells in 10cm dish. The following day, supernatant of R7f and Rec5 virus were infected into NIH3T3 cells at m.o.i 1. From 1 d.p.i. to 5 d.p.i., cells were harvested and downstream assay were performed accordingly.

- **Focal Immunoassay**

Virus titer was determined by infecting M. dunni cells at 2×10^4 cells in 3.5-cm dish of 6 well plates. The next day, virus supernatant of dilution 1/10, 1/100 and 1/1000 were infected into the cells in the presence of 10 µg/ml polybrene (Czub et al., 1991). Supernatants were refreshed daily, and titration was done on 5 d.p.i.. Env protein on cell surface was stained with monoclonal antibody 85-1 (Ikeda et al., 1995). Cells were fixed in 0.5% glutaraldehyde and horse

peroxidase-conjugated sheep anti-Mouse IgG whole antibody (GE Healthcare) was used as secondary antibody.

- **Immunoblot analysis**

Western blot analysis was performed on R7f and Rec5 infected over a time course study. Cells were washed with PBS and then lysed with 2% sodium dodecyl sulphate (SDS) and 0.5 mM phenyl methyl sulfonyl fluoride (PMSF) and boiled for 5 minutes. Nucleic acids were sheared using 23G-needle. Sample buffer (5x) containing SDS, dithiothreitol (DTT), glycerol, and bromophenol blue in Tris-HCl (pH 6.8) was added to the lysate. After boiling for 5 minutes, the lysates were loaded onto a 5% SDS-polyacrylamide gel and electrophoresed. The proteins were then transferred onto an Immobilon P membrane (Milipore) by electroblotting. To detect the Env protein and Gag protein, goat anti-Rauscher MLV gp70 and anti-AKR p30^{Gag} (Quality Biotech Incorporated Resource Laboratory) was used. Actin was detected using rabbit anti-beta-actin (Santa Cruz Biotechnology) as a loading control. Horseradish peroxidase-conjugated anti-goat IgG antibody and anti-rabbit IgG (Santa Cruz Biotechnology) were used as a second antibody. The membrane was developed with ECL plus reagents (Amershan Bioscience Corp.). These bands were visualised with Image Master VDS-CL and quantified using ImageJ software.

- **RNA extraction and quantification**

RNA extraction was carried out using an RNase Mini Kit (Qiagen). RNA was treated with RNase-free DNase (Qiagen) and 2ug of RNA were reverse transcribed using an OligodT₂₀ primer and SSIII reverse transcribing kit (Invitrogen). A portion of the resulting cDNA was subjected to real-time PCR using an Applied Biosystems® 7500 Real-Time PCR System. The specific primers and probes used for detection of total viral mRNA were as follows: forward primer Env-F (AGGACCTCGGGTCCCAATAG), reverse primer Env-R (TTAGGTAGCGGGAACGAAAGTT),

and the TaqMan probe: CCGAACCCCGTCCTGGCAGAC. Spliced viral-mRNA was detected using s6 (GGGTCTTTCATTTGGGGGCTC), s2 (TGCCGCCAACGGTCTCC), and the TaqMan probe (CACCACCGGGAGCTCATTTACAGGCAC). Standard curves to quantify both mRNAs derived from the luciferase expression vectors utilized vector splA8L (Yamamoto and Takase-Yoden, 2009). The Ct (threshold cycle) values for all standard curves were produced within 13 to 35 cycles of amplification. Ct values that fell within the range of the standard curve were used for quantifying the sample mRNA. In addition, *gapdh*-mRNA was quantified as an internal control using TaqMan Rodent GAPDH Control Reagents with the primer sets and probes supplied by the manufacturer (Applied Biosystems). Standard curves to calculate the amount of mRNA were generated using serially diluted *gapdh* T-easy vector. Negative control samples in which the cDNA synthesis step was omitted, showed undetectable levels of amplification.

- **Genomic DNA extraction and quantification**

Cellular genomic DNA (gDNA) was extracted using a DNeasy Blood and Tissue Kit (Qiagen) according to the manufacturer's instructions. Real-time PCR was performed to quantify the amount of viral DNAs using the following primers and probe: forward primer Env-F (AGGACCTCGGGTCCCAATAG), reverse primer Env-R (TTAGGTAGCGGGAACGAAAGTT), and the TaqMan probe (CCGAACCCCGTCCTGGCAGAC). introduced into the cells. The amount of *gapdh* DNA was measured as an internal control using the TaqMan Rodent GAPDH Control Reagents.

❖ Results

This study is based on a background study which revealed that the 0.3-kb KpnI-AatII fragment containing the R-U5-5' leader sequence was essential for the induction of spongiform neurodegeneration and for the up-regulation of Env protein expression (Takase-Yoden and Watanabe, 2005). Within the 0.3-kb fragment, 17 nucleotides differ between A8 and 57 sequences (Fig. 1-1). The effect of the 0.3-kb fragment was studied based on two chimeric viruses, Rec5 and R7f where each carries the 0.3-kb fragment of 57 and A8 respectively and an A8-*env* gene (Fig 1-2). First, the effect of the 0.3 kb fragment on viral growth was determined. As shown in Fig. 1-3, a viral titer of about 10^4 was achieved at 1 day post-infection (dpi) for both R7f and Rec5. The viral titer increased to above 10^6 at 2 dpi and reached a lag phase from 3 dpi onwards. There was no difference in the level of viral production between R7f and Rec5 throughout the 5 days of incubation.

Next, we performed an immunoblot analysis to determine the amount of viral protein in NIH3T3 cells over a 5 day incubation period. Significantly greater amounts of Env protein were present in R7f-infected cells at 2 dpi compared to Rec5-infected cells (Fig. 1-4A). In contrast, the amount of Gag protein in R7f-infected cells was similar to that in Rec5-infected cells (Fig. 1-4B). These results are in agreement with those reported previously for rat glial cells F10 (Takase-Yoden and Watanabe, 2005). The amounts of Env and Gag proteins at 1, 3, and 5 dpi were determined by measuring the intensity of the band from the western blot membrane and normalised against the intensity of β -actin and the amount of viral DNA in the infected cells (Table 1-1). The amounts of Env and Gag proteins are shown relative to those in R7f-infected cells at 1 dpi. The relative amount of Env in R7f-infected cells was 1.0, 8.3 and 10.3 at 1, 3, and 5 dpi respectively. In Rec5-infected cells, the relative amount of Env was 0.5, 1.9 and 3.1 at 1, 3, and 5 dpi respectively. Thus, Env expression in R7f was 3- to 4-fold higher than that of Rec5 at 3 dpi ($p < 0.05$) and 5 dpi ($p < 0.005$).

```

A8 1  GCGCCAGTCC TCCGACAGAC TGAGTCGCCG KpnI 1 2 3 polyA 4
57 1  ***** T***** ***** GGTACCGT GTATCC AATA AATCCTCTTG
                    *****T***** ***** A*TC***** *G*****

A8 61  CTGTTGCARTC U5 5 CGACTTGTGG TCTCGCTGTT CCTTGGGAGG GTCTCCTCAG AGTGATTGAC
57 61  ***** C***** ***** ***** ***** *****

A8 121 TACCCGTCTC GGGGGTCTTT U5 5'leader PBS 6 7
57 121 ***** ***** *****T***** *****T***** *****A

A8 181 GGACCACCGA CCCACCACCG 5'ss GGAGGTAAGC 8 TGCCAGCAA TTGATCGGTG TCTGTCCATT
57 181 ***** ***** *****T***** *****T***** *****

A8 241 GTCCCGTGTC 9 10 11 12
57 241 ***** T***** *T***** *C*T***** *****

A8 301 13 14 15 16 17 Glyco-Gag start
57 301 GTATCTGGCG GACCCGTGGT AGAACTGACG AGTTCGGGAT ACCCGGCCGC AACCTGGGA
                    ***C***** ***** G***** G*****A**C ***** *****

A8 361 AatII
57 361 GACGTCCCAG G
                    ***** *

```

Figure 1-1

Alignment of the 0.3-kb KpnI-AatII fragment of A8 (accession no. D88386) and 57 (accession no. X02794). Asterisks represent the sequence identity. PolyA: polyadenylation signal; PBS: primer binding site; 5'ss: 5' splice site; glyco-Gag start; the start codon of glycosylated-Gag protein. Different nucleotides between A8 and 57 within the 0.3-kb fragment are numbered.

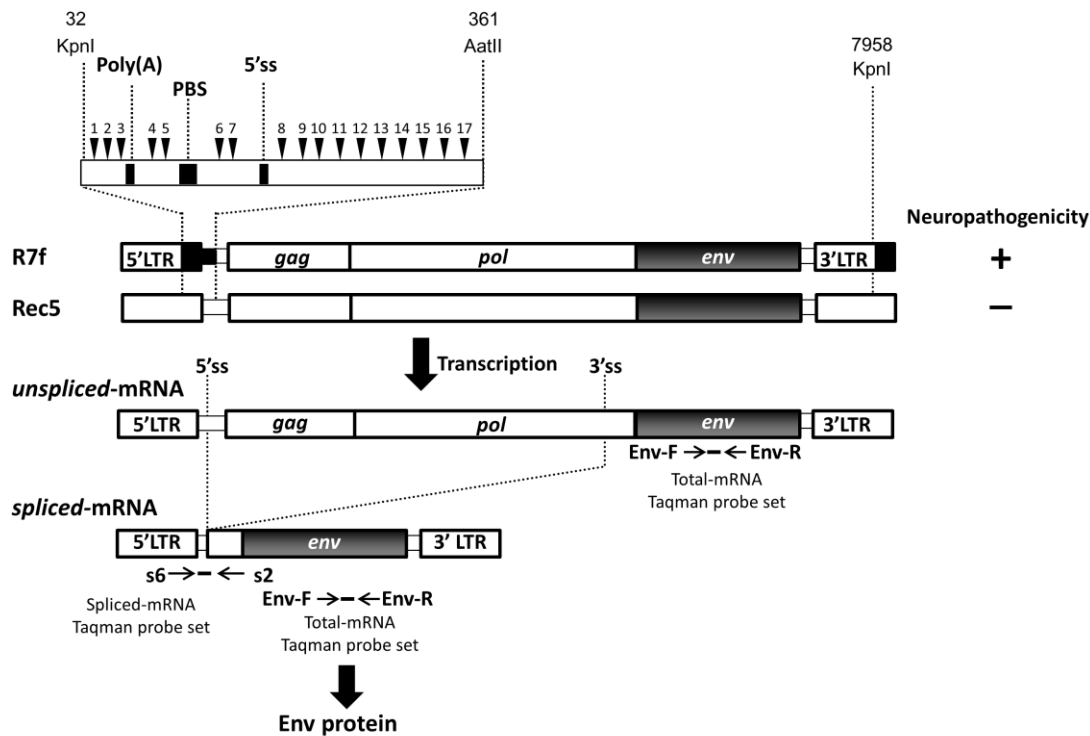


Figure 1-2

Structures of the R7f and Rec5 viruses. In the viral genomes, solid regions indicate sequences derived from the A8 virus and open region show sequences derived from the clone 57 virus. The numbering of the nucleotides is based on the transcript. The primers and probes used for RT-PCR to detect the corresponding mRNA are shown. The inset shows the 0.3-kb KpnI-AatII fragment. Nucleotides marked by numbered black triangles are those that differ between clones A8 and 57. The following functional domains are indicated: Poly (A), polyadenylation signal; PBS, primer binding site; 5'ss, 5' splice site.

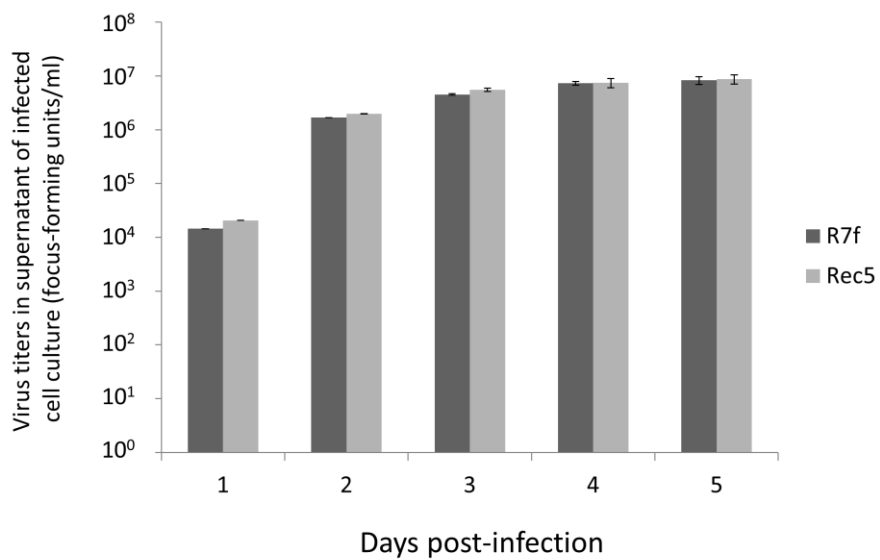


Figure 1-3

Viral titers in cultured supernatants of cells infected with R7f or Rec5. Viral titers from 1 to 5 dpi were determined by focal immunoassays using *Mus dunnii* cells. The graphs represent the average value (\pm SEM) of four independent experiments.

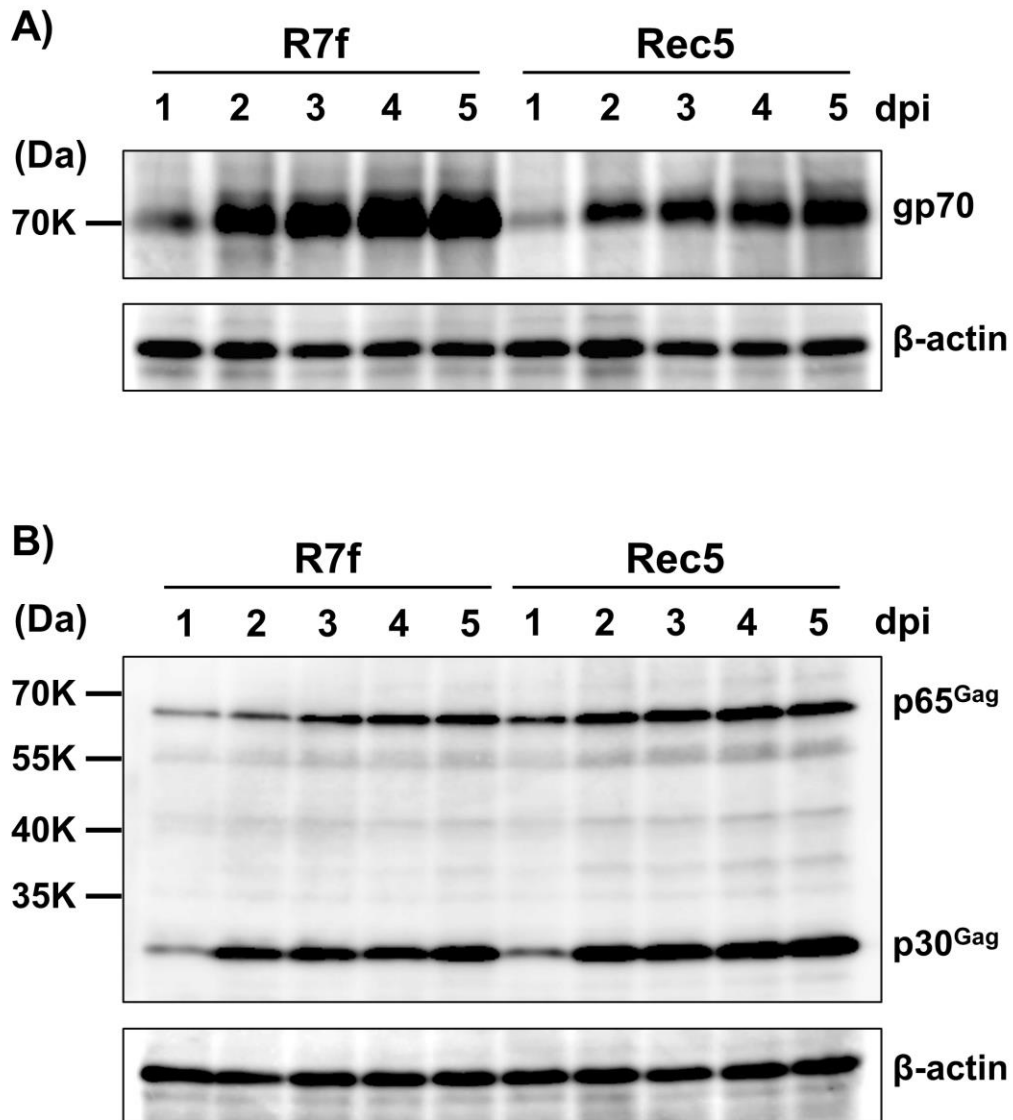


Figure 1-4

Expression of Env protein (A) and Gag protein (B) in NIH3T3 cells infected with R7f or Rec5. Lysates from the infected cells were analyzed by immunoblotting with anti-Env (gp70) and anti-Gag (p30) antibodies. p65^{Gag}, Gag precursor protein. After reprobing, the blot was subsequently stained using anti-β-actin antibody to control for loading differences. This figure is representative of the results obtained. Experiments were performed using three independent samples and similar results were obtained.

By contrast, the relative amount of Gag in R7f-infected cells was 1.0, 2.9, and 4.1 at 1, 3, and 5 dpi respectively. In Rec5-infected cells, the relative amount of Gag was 1.1, 2.4 and 3.0 at 1, 3, and 5 dpi respectively. There was no significant difference in the amount of Gag protein between R7f and Rec5.

The effect of the 0.3 kb fragment on mRNA expression levels was also determined. First, total viral mRNA of both viruses was measured by real-time RT-PCR using Env-F and Env-R primers (Fig. 1-2) and normalized against the amount of *gapdh*-mRNA and viral DNA. We found that total viral mRNA was similar in R7f- and Rec5-infected cells over the course of the observation period (Fig. 1-5A). Next, we measured spliced *env*-mRNA levels by real-time RT-PCR using s6 and s2 primers (Fig. 1-2), which amplify a fragment containing the splicing junction from the cDNA of spliced transcripts; *env*-mRNA levels were normalized as described above. The amounts of spliced *env*-mRNA of R7f and Rec5 were identical at 1 dpi. However, the amount of spliced *env*-mRNA of R7f increased to about double that of Rec5 at 3 dpi ($p < 0.01$) and at 5 dpi ($p < 0.005$) (Fig. 1-5B). The ratio of the amount of spliced *env*-mRNA to total viral mRNA was estimated as 0.06, 0.14 and 0.13 in R7f-infected cells at 1 dpi, 3 dpi and 5 dpi, respectively, on the basis of the copy number of *env*-mRNA and total viral mRNA (Table 1-1). In contrast, the ratios in Rec5-infected cells were 0.06, 0.08 and 0.07 at 1 dpi, 3 dpi and 5 dpi, respectively. Thus, the ratio of abundance of spliced *env*-mRNA in R7f-infected cells was about double that in Rec5-infected cells at 3 dpi ($p < 0.01$) and at 5 dpi ($p < 0.01$).

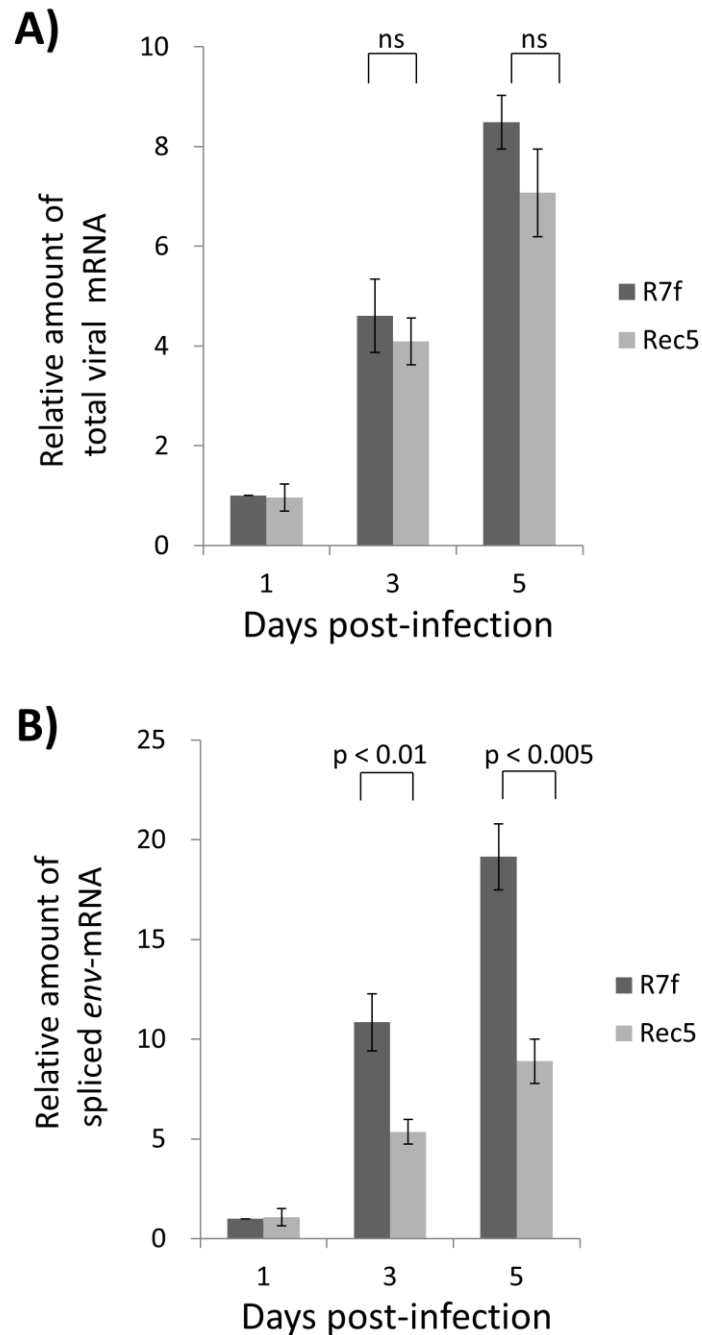


Figure 1-5

Relative amounts of total viral mRNA (A) and spliced *env*-mRNA (B). Total RNA extracted from NIH3T3 cells infected with R7f or Rec5 were subjected to first strand cDNA synthesis. The amount of mRNA was measured using real time PCR and the value was normalized against the amount of *gapdh*-mRNA and viral DNA. The amount shown is relative to the amount of R7f on 1 dpi. The graphs represent the average value (\pm SEM) of four independent experiments. Statistical comparisons were performed using the t test; ns, differences were not significant.

Virus	dpi	Relative amount ^a of		Copy number ^b of		The ratio ^c of <i>env</i> -mRNA per total viral mRNA
		Env protein	Gag protein	<i>env</i> -mRNA	total viral mRNA	
R7f	1	1.0 ± 0.0	1.0 ± 0.0	1.6 ± 0.3 × 10 ⁴	2.9 ± 0.6 × 10 ⁵	0.06 ± 0.00
	3	8.3 ± 2.3*	2.9 ± 0.3	1.7 ± 0.4 × 10 ⁵	1.4 ± 0.5 × 10 ⁶	0.14 ± 0.02**
	5	10.3 ± 1.2**	4.1 ± 0.9	3.0 ± 0.4 × 10 ⁵	2.4 ± 0.5 × 10 ⁶	0.13 ± 0.01****
Rec5	1	0.5 ± 0.1	1.1 ± 0.3	1.6 ± 0.5 × 10 ⁴	2.6 ± 0.7 × 10 ⁵	0.06 ± 0.01
	3	1.9 ± 0.2	2.4 ± 0.6	7.4 ± 1.8 × 10 ⁴	1.1 ± 0.3 × 10 ⁶	0.08 ± 0.01
	5	3.1 ± 0.7	3.0 ± 1.0	1.4 ± 0.2 × 10 ⁵	2.0 ± 0.4 × 10 ⁶	0.07 ± 0.01

Table 1-1

Comparison of viral protein expression levels, *env*-mRNA and total viral mRNA levels, and the ratios of the amount of *env*-mRNA to that of total viral mRNA.

Statistical comparisons were performed using the t test.

* $p < 0.05$ vs Env of Rec5 at 3 dpi, ** $p < 0.005$ vs Env of Rec5 at 5 dpi, *** $p < 0.01$ vs the ratio of Rec5 at 3 dpi, **** $p < 0.01$ vs the ratio of Rec5 at 5 dpi.

^a Means (\pm SEM) of three independent experiments are shown.

^b Means (\pm SEM) of four independent experiments are shown. For quantification of the amount of mRNA, 2 μ g of total mRNA of virus-infected cells were used for reverse transcription. An aliquot (1/200) of the cDNA sample was subjected to real-time PCR analysis. The copy number of *env*-mRNA and total viral mRNA was normalized against the amount of *gapdh*-mRNA and viral DNA.

^c Ratio in each of four independent experiments was calculated; the mean ratio (\pm SEM) is shown.

❖ Discussion

The contribution of the 0.3-kb fragment of clone A8 to the increase in the expression level of Env protein was demonstrated in our previous studies (Takase-Yoden et al., 2006; Takase-Yoden and Watanabe, 2005). In the present study, we sought to understand the role of the 0.3-kb fragment in Env protein expression by investigating various stages of viral growth. By comparing R7f and Rec5, the 17 nucleotides difference in the 0.3-kb fragment had no effect on viral production (Fig. 1-3), the level of expression of the Gag protein (Fig. 1-4B and Table 1-1), or the amount of total viral mRNA (Fig. 1-5A). However, the 0.3-kb fragment of clone A8 showed about a 2-fold increase in the amount of spliced *env*-mRNA (Fig. 1-5B). This result differs from that obtained in our previous study, which found little difference in the amount of spliced *env*-mRNA in R7f-infected cells and Rec5-infected cells (Takase-Yoden and Watanabe, 2005). The amounts of mRNA were measured in the previous work using band intensities on electrophoresis gels in the linear range of the PCR amplification; the current protocol measured viral mRNA levels using real-time RT-PCR. The difference between the studies might be due to the increased sensitivity of the real-time RT-PCR method.

The increase in the amount of spliced *env*-mRNA was consistent with the increase in the amount of Env protein in R7f-infected cells throughout the 5 day period after infection. However, neither viral production nor total viral mRNA was consistent with the level of Env protein in R7f-infected cells. Therefore, we suggest that the 0.3-kb fragment influences the level of Env protein by regulating the amount of spliced *env*-mRNA rather than of total viral mRNA or viral production. The ratio of the amount of spliced *env*-mRNA to the amount of total viral mRNA in R7f-infected cells was about 2-fold higher than that in Rec5-infected cells (Table 1-1). This fact suggests that the 0.3-kb fragment might influence splicing efficiency. Other studies have shown that region around the 5' splice site forms a secondary structure, which has been determined in part by chemical probing and functional analysis; formation of the secondary structure may regulate

splicing by modulating accessibility to splicing factors (Kraunus et al., 2006; Zychlinski et al., 2009). Another possibility is that the 0.3-kb fragment might also influence other post-transcriptional processes such as poly (A) tail processing, nuclear-cytoplasmic transport of mRNA, and ribosome recycling during the translation step. Indeed, the amount of spliced *env*-mRNA in R7f-infected cells was 2-fold higher than that in Rec5-infected cells, whereas the amount of Env protein in R7f-infected cells was 3- to 4-fold higher than in Rec5-infected cells. To fully elucidate the role of the 0.3-kb fragment in Env protein expression, analysis using a vector containing the 0.3-kb fragment and a reporter gene will be of value.

In the present study, we showed that the 0.3-kb fragment influenced the expression level of the Env protein by regulating the amount of spliced *env*-mRNA in cultured cells. This finding supports our proposal that the A8-derived 0.3-kb fragment increases the expression level of the Env protein in brains of infected rats and that the high expression level of the Env protein is correlated with neuropathogenicity (Takase-Yoden et al., 2006; Takase-Yoden and Watanabe, 2005; Watanabe and Takase-Yoden, 2006). In a previous study, we examined the effect of the A8-derived 0.3-kb fragment on the neuropathogenicity of chimeric viruses that had A8-*env* on a 57 background (Takase-Yoden et al., 2006; Takase-Yoden and Watanabe, 2005). R7a virus, which has the A8 sequences from the U3 of the LTR to the end of the 0.3 kb fragment and has A8-*env* on a 57 background, showed neuropathogenicity. By contrast, the R7g virus, in which the 0.3-kb fragment of R7a is replaced by a 57-derived 0.3-kb fragment, did not show neuropathogenicity (Takase-Yoden and Watanabe, 2005). This finding reaffirmed the contribution of the 0.3 kb fragment to neuropathogenicity. However, as the *gag* and *pol* genes of R7g are of 57 origin, then constructing a chimeric virus that contains the 57-0.3 kb on a complete background of A8 sequences may help to clarify the importance the 0.3-kb fragment in inducing neuropathogenicity. Additionally, a reverse chimeric virus that carries the A8-0.3 kb fragment on a complete background of 57 sequences may help to elucidate whether or not the A8-0.3 kb fragment increases the expression

level of the 57-Env protein. Our previous studies showed that the Rec6 virus, which has the *57-env* on a background of A8 sequences, could proliferate well in rat brains but did not induce spongiform neurodegeneration (Takase-Yoden and Watanabe, 1997). This suggested that the 57-Env protein was not able to induce spongiosis. However, it is not clear whether a chimeric virus that has the A8-0.3 kb fragment on a complete background of 57 shows neuropathogenicity. Therefore, we hope to ascertain the effect of the 0.3-kb fragment on the expression level of Env and neuropathogenicity by testing these chimeric viruses.

CHAPTER 2

Mechanism by which the 0.3-kb fragment participates in protein expression

❖ Materials and Methods

• Vector construction

Luciferase expression vectors R7f-L and Rec5-L were constructed as described previously by replacing the viral *env* gene with the *luc* gene (Yamamoto and Takase-Yoden, 2009) within its proviral sequences (Takase-Yoden and Watanabe, 2005). The point mutations G to T (2608nt), G to T (2614nt), and G to T (2629nt) were introduced into the *pol* gene of each recombinant plasmid. R7fa-L was constructed by replacing the 57 sequences of KpnI (32) and AatII (361) with the A8 sequences in Rec5-L. R7fb-L was generated by replacing the A8 sequences of KpnI (32) and AatII (361) with the 57 sequences in R7f-L. Mutation vector F1-L was constructed by mutagenesis of R7f-L using the following forward primer: CGCCCGGGTACCCGTATTCCCAATAAAGCCTCTTGCTG; and the reverse primer: ACGGGTACCCGGGCGACTCAGTCTA. F2-L was generated by mutagenesis of F1-L using the forward primer: TCTTGCTGTTGCATCCGACTCGTGGTCTCGCTGTT; and the reverse primer: AGTCGGATGCAACAGCAAGAGGCTTTATTG. F3-L was constructed by mutagenesis of F2-L using the forward primer: TTTGGGGGCTCGTCCGGGATCTGGAGACCCTTGCCCAAGGACCACCGA; and the reverse primer: GATCCCGGACGAGCCCCCAAATGAAAGACCC. F4-L was generated by mutagenesis of F3-L using the forward primer: AAGCTGGCCAGCAATTGATcGTGTCTGTCC; and the reverse primer: GATCAATTGCTGGCCAGCTTACCTCCCGGT. B1-L was generated by mutagenesis of R7f-L using the forward primer: ACCCGTGGTAGAACTGACGGGTTTCGAGACACCCGGCCGCAA; and the reverse primer:

CGTCAGTTCTACCACGGGTCCGCCAGATA. B2-L was generated by mutagenesis of B1-L using the forward primer: TTGGCCGACTAGCTCTGTACCTGGCGGACCCGTGGTGGAACTGACG; and the reverse primer TACAGAGCTAGTCGGCCAACTAGTACAGAC. B3-L was generated by mutagenesis of B2-L using the forward primer: CCATTGTCCCGTGTCTTTGATTGATTTTATGCGCCTGCGTTTGTACTAGT; and the reverse primer: TCAAAGACACGGGACAATGGACAGACACCG. R7f.5m-L was constructed by mutagenesis of R7f-L using the forward primer: TCTTGCTGTTGCATCCGACTCGTGGTCTCGCTGTT; and the reverse primer: AGTCGGATGCAACAGCAAGAGGATTTATTG. R7f.567m-L was constructed by mutagenesis of R7f.5m-L using the forward primer: TTTGGGGGCTCGTCCGGGATCTGGAGACCCTTGCCCAAGGACCACCGA; and the reverse primer: GATCCCGGACGAGCCCCAAATGAAAGACCC. Rec5.5m-L was constructed by mutagenesis of Rec5-L using the forward primer: TCTTGCTGTTGCATCCGACTTGTGGTCTCGCTGTT; and the reverse primer: AGTCGGATGCAACAGCAAGAGGCTTTATTG. Rec5.567m-L was constructed by mutagenesis of Rec5.5m-L using the forward primer: GGAGACCCTTGCCCAGGGACCACCGACC; and the reverse primer: AAGGGTCTCCGGATCCCGGACGAGCCC. Structures of the expression vectors were confirmed by digestion with restriction enzymes and sequence analysis. Basic recombinant DNA procedures were performed according to standard protocols (Sambrook, 1989).

- **Cell culture**

NIH3T3 cells were grown in Dulbecco's Modified Eagle Medium – low glucose (SIGMA) supplemented with 10% fetal calf serum (MP Biomedicals) and penicillin-streptomycin (GIBCO) and cells were incubated at 37°C in a 7% CO₂ atmosphere. HeLa cells were grown under the

same conditions as NIH3T3 except they were incubated in a 5% CO₂ atmosphere.

- **Transfection and assay for luciferase activity**

NIH3T3 cells (1×10^5) were plated in 24-well plates with growth medium minus penicillin and transfected the next day with 0.8 ug luciferase expression vectors, 5 ng of pRL-SV40 (Promega) using 2ul of Lipofectamine 2000 Reagent (Invitrogen, Carlsbad, CA, USA) diluted with OPTI-MEM (Invitrogen). After 48 hours, cells were lysed and luciferase activities were measured as Relative Light Units (RLU) using a luminometer with a Dual-Luciferase Reporter Assay System (Promega) according to the manufacturer's instructions. The luciferase activity of each sample was normalized to that of Renilla (pRL-SV40) as an internal control.

- **RNA extraction and quantification**

RNA extraction was carried out using an RNase Mini Kit (Qiagen). RNA was treated with RNase-free DNase (Qiagen) and 2ug of RNA were reverse transcribed using an OligodT₂₀ primer and SSIII reverse transcribing kit (Invitrogen). A portion of the resulting cDNA was subjected to real-time PCR using an Applied Biosystems® 7500 Real-Time PCR System. The specific primers and probes used for detection of total mRNA at the *luc* region were: LucF: CGGCTTCGGCATGTTCA; LucR: TACATGAGCACGACCCGAAA; TaqMan probe: CACGCTGGGCTACTTGATCTGCGG. *Spliced*-mRNA was detected using s6: GGGTCTTT CATTGGGGGCTC; s2: TGCCGCCAACGGTCTCC and the TaqMan probe: CACCACCGGGAGCTCATTACAGGCAC. Standard curves to quantify both mRNAs derived from the luciferase expression vectors utilized vector splA8L (Yamamoto and Takase-Yoden, 2009). In addition, *gapdh*-mRNA was quantified as an internal control using TaqMan Rodent GAPDH Control Reagents containing primer sets and probes (Applied Biosystems). Standard curves to calculate the amount of mRNA were created using serially diluted *gapdh* T-easy vector. The

negative control samples without the cDNA synthesis step showed undetectable amplification.

- **Genomic DNA extraction and quantification**

Cellular genomic DNA (gDNA) was extracted using a DNeasy Blood and Tissue Kit (Qiagen) according to the manufacturer's instructions. Real-time PCR was performed to quantify the amount of plasmid DNAs introduced into the cells. Primers and probe sets used to quantify the amount of firefly luciferase expression vector introduced were the same TaqMan primer and probe set used to detect the amount of cDNA. The amount of *gapdh* DNA was measured as an internal control using the TaqMan Rodent GAPDH Control Reagents.

- **Cell fractionation**

Nuclear and cytoplasmic fractions were obtained from cultured cells using a PARIS kit (Ambion) according to the manufacturer's manual. As a control for the fractionation, an aliquot of total RNA from each section was electrophoresed on a 1% agarose gel in morpholinepropane-sulfonic acid (MOPS) buffer, and the cellular ribosomal RNAs were visualized by ethidium-bromide staining.

- **Determination of poly (A) tail length**

Total RNA extracted from 24 hours post-transfected HeLa-cells were ligated with RV3PC-anchor primers. Reverse transcription was then carried out using an antisense sequence of the RV3PC-anchor primer. To amplify the poly (A) tail of mRNA, a forward primer targeting the 3'end of U3 at LTR (AGCTCACAACCCCTCACTCGGC) was paired with a reverse primer targeting the RV3PC-anchor sequence. To increase the likelihood of the reverse primer binding at the poly(A) tail, ten thymines were added into the 3'end of the reverse primer sequence (CTAGCAAATAGGCTGTCCCTTTTTTTTTT). Likewise, to detect the poly (A) tail length of

the *gapdh*-mRNA, a forward primer, Mgapdh3end (CCCTACTCTCTTGAATACCATCA), was set at the junction before the poly(A) signal and was used with the same reverse primer targeting the RV3PC-anchor sequence. The resulting PCR products were stained in ethidium bromide and electrophoresed on an 8% polyacrylamide gel to visualize the spliced mRNA. A 3% agarose gel was used to visualize *gapdh*-mRNA. Within the pool of reverse-transcribed cDNA, the following primers were used to detect the presence of *luc*-mRNA: forward primer f-597 (GGGCTCGTCCGGGATC) and reverse primer s2 (TGCCGCCAACGGTCTCC); for *gapdh*-mRNA, the forward and reverse primers from the Taqman Rodent GAPDH control reagents (Applied Biosystems) were used.

❖ Results

The 0.3-kb fragment effects on luciferase protein expression and the amount of spliced *luc*-mRNA

The purpose of the present study is to further investigate the function of the 0.3-kb fragment in retroviral gene expression. Between the A8 and 57 sequences within the 0.3-kb fragment, 17 nucleotides differ (Fig. 1-1). To investigate the function of the 0.3-kb fragment in viral gene expression, the full-length viral genomes of Rec5 and R7f were recombined with the *luc* gene, in which the viral *env* gene was replaced with the *luc* gene to produce the luciferase expression vectors Rec5-L and R7f-L, respectively (Fig. 2-1). Both Rec5-L and R7f-L were constructed using the complete virus 57 sequences, however, in R7f-L the 0.3-kb fragment was derived from the viral A8 sequence. The luciferase protein is translated from spliced mRNA of these expression vectors. After transfection of the vectors into NIH3T3 cells, luciferase activities were measured. The luciferase activity of R7f-L increased by 2-fold compared to that of Rec5-L ($p < 0.001$) (Fig. 2-2A). To determine the role of the 0.3-kb fragment positioned at the 5'LTR-leader sequence and the 3'LTR in the expression vectors, R7fa-L and R7fb-L were constructed (Fig. 2-1). R7fa-L, which carries the 0.3-kb fragment of A8 only at the 5'LTR-leader sequence, exhibited the same amount of luciferase activity as R7f-L, and the luciferase activity of R7fb-L, which carries the 0.3-kb fragment of A8 only at the 3'LTR, showed luciferase activity that was lower compared to R7fa-L ($p < 0.005$) and comparable to that of Rec5-L (Fig. 2-2A).

Furthermore, the effect of the 0.3-kb fragment on the *luc*-mRNA level was also determined. The spliced *luc*-mRNA levels were measured by real-time RT-PCR using s6 and s2 primers (Fig. 2-1). These primers were designed to amplify a fragment containing the splicing junction region from the cDNA of spliced transcripts. The amount of spliced *luc*-mRNA from R7f-L increased by 2-fold compared to that from Rec5-L ($p < 0.001$) (Fig. 2-2B). The amount of spliced *luc*-mRNA from R7fa-L was the same as that from R7f-L. The amount of spliced *luc*-mRNA from

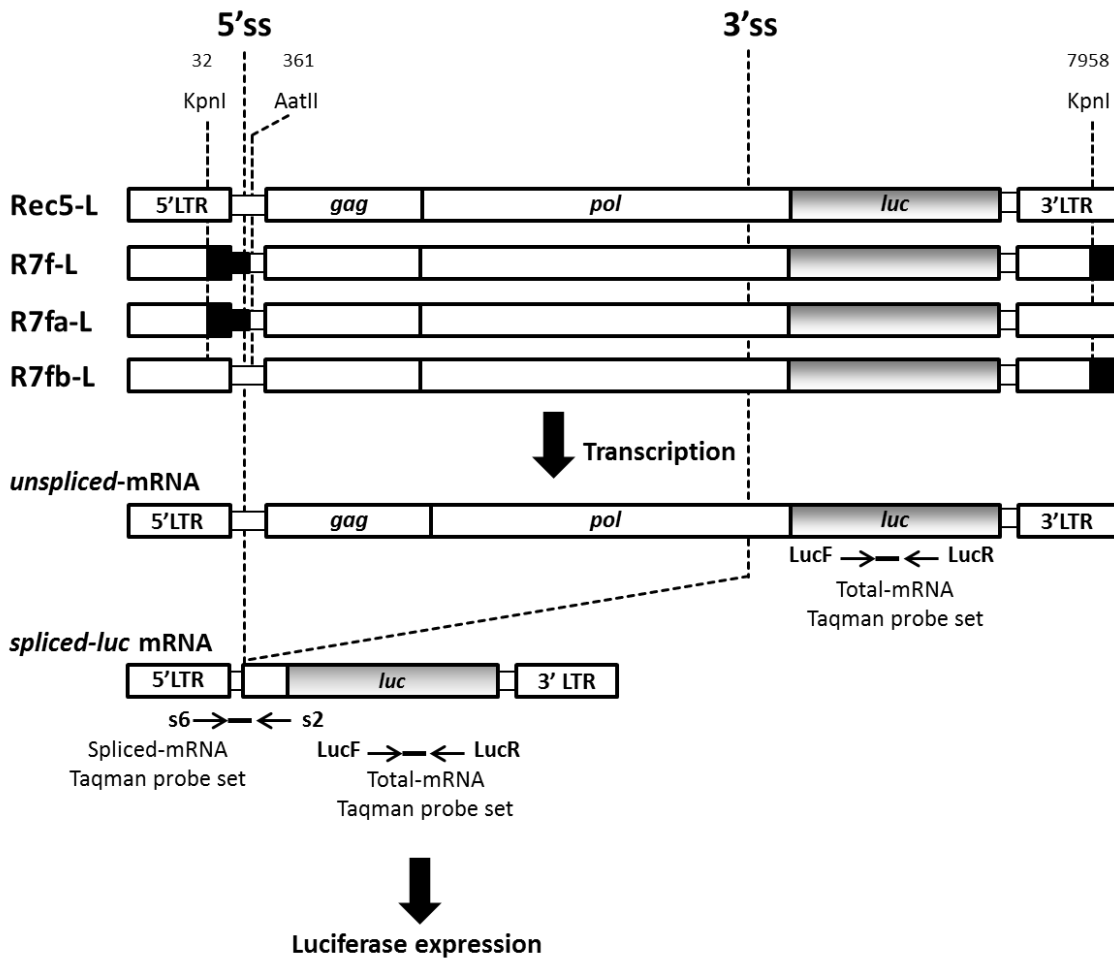


Figure 2-1

Structures of luciferase expression vectors. In the viral genomes, solid regions are sequences derived from the A8 virus and open regions are sequence derived from the 57 virus. The numbering of nucleotides is based on the transcript. Vectors and primers and probes used to detect the corresponding mRNA by RT-PCR are indicated on the vectors. 5'ss: 5' splice site; 3'ss: 3' splice site.

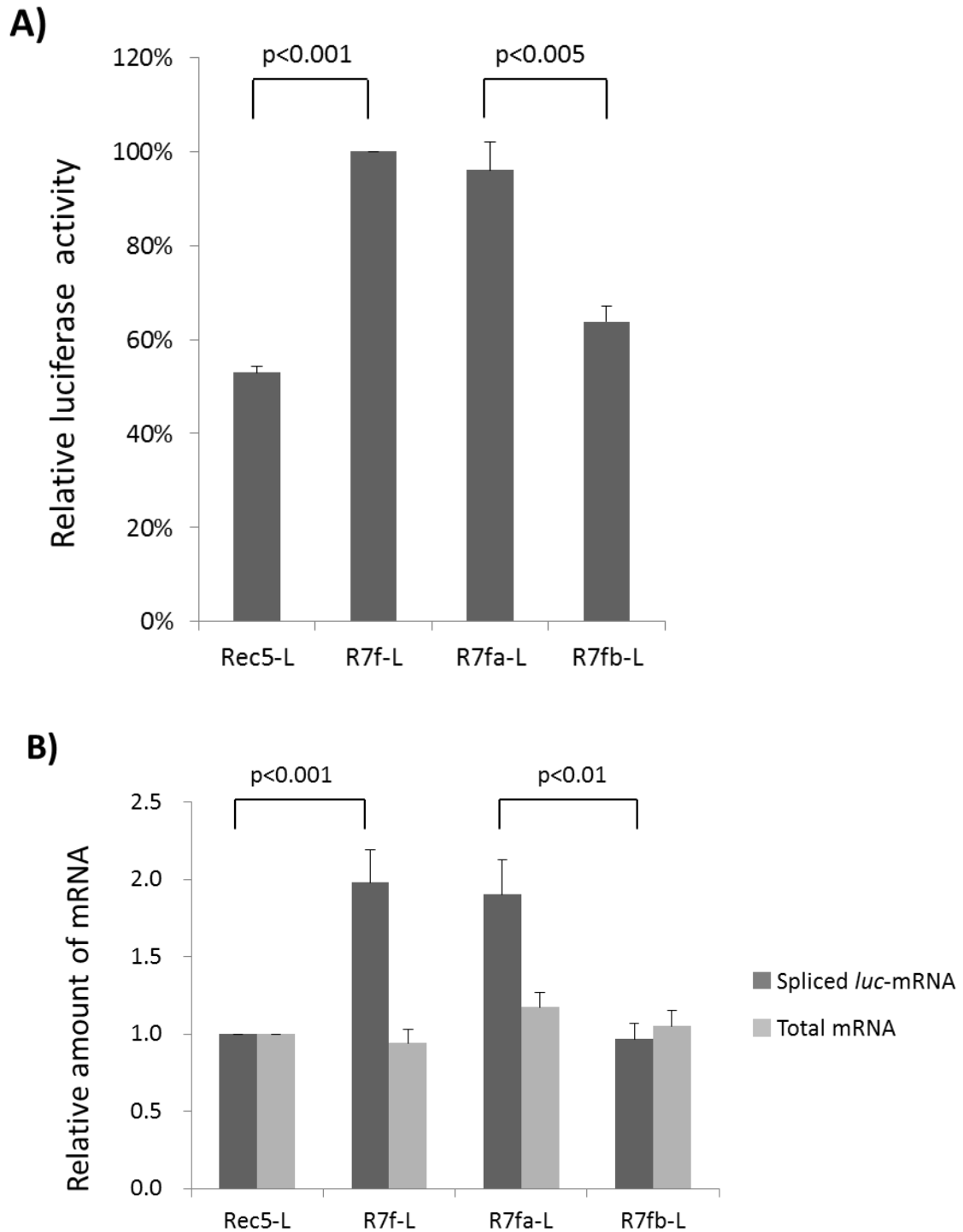


Figure 2-2

Relative Luciferase activity (A) and relative amount of total mRNA and spliced *luc*-mRNA (B). The graphs show the mean values from 4-7 independent results and SEM are shown. The statistical comparison was done using the *t* test, ns: differences were not significant.

R7fb-L was lower than that from R7fa-L ($p < 0.01$) but was comparable with that from Rec5-L (Fig. 2-2B). The amount of spliced mRNAs paralleled the luciferase activity. Next, to examine effects of the 0.3-kb fragment on transcriptional activity, the amount of total transcripts from expression vectors were measured by real-time RT-PCR using the LucF and LucR primers (Fig. 2-1). The amounts of total mRNA measured for all of the expression vectors were comparable (Fig. 2-2B).

The 0.3-kb fragment did not affect the poly (A) tail length of mRNA or the nuclear-cytoplasmic distribution of *luc*-mRNA

In general, the poly (A) tail length of mRNA is correlated with the efficiency of translation. Therefore, to examine whether or not the 0.3-kb fragment influences polyadenylation of viral mRNA, the poly (A) tail lengths of mRNA from Rec5-L and R7f-L transfected Hela cells were compared. Total RNA was harvested and anchored with the RVP3 primer before the first strand of cDNA was synthesized with an anti-RVP3 oligo strand. To determine the poly (A) tail length, the transcripts derived from Rec5-L and R7f-L were selectively amplified using the forward primer for viral U3 sequences of the 3'LTR and the reverse primer for the RVP3 sequence. PCR products viewed on electrophoresed gels showed no detectable differences in the smeared patterns indicating the poly (A) tail lengths of transcripts derived from R7f-L and Rec5-L (Fig. 2-3). In this system, the poly (A) tail lengths of transcripts containing both the unspliced mRNA and the spliced mRNA derived from the vectors could be detected. Therefore, to confirm that the first strand of cDNA synthesized with an anti-RVP3 oligo strand contained spliced-mRNA, from which luciferase protein was translated, PCR was performed using the primer set of f-597 and s2. As shown in figure 2-3, a 113-bp band that came from spliced-mRNA was detected in both Rec5-L and R7f-L transfected cells. As a control, the poly (A) tail length of *gapdh*-mRNA was examined in Rec5-L and R7f-L transfected cells. In both of these cells, a 177-bp band for *gapdh*-mRNA was detected, and there were no detectable differences in the smeared patterns indicating the poly (A) tail length of

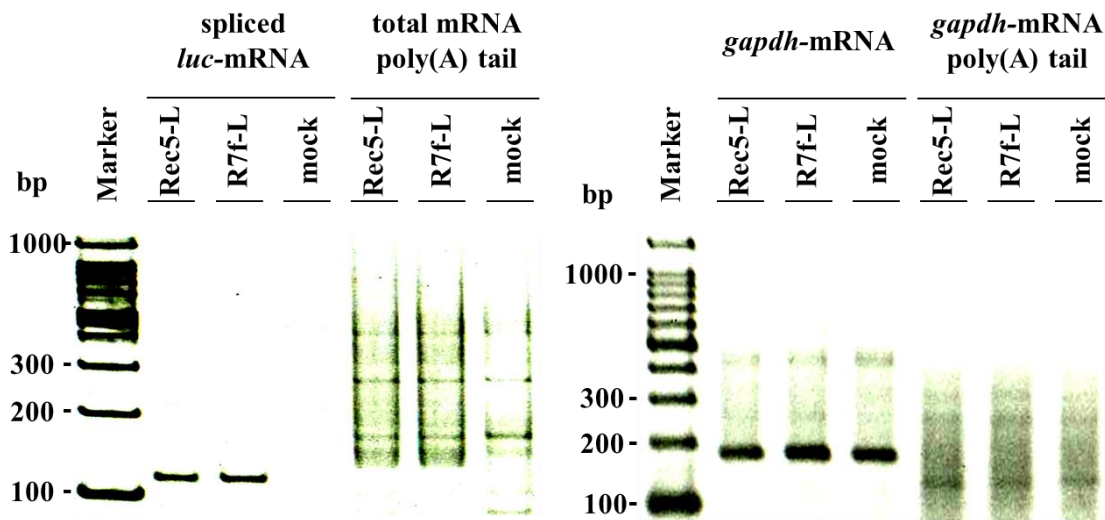


Figure 2-3

Determination of poly (A) tail length. Total RNAs extracted from 24 hours post-transfected Hela-cells were ligated with the anchor primer RVP3 oligo. First strand cDNA synthesis was carried with an antisense sequence to the anchor primer. To detect poly (A) tail length, the transcripts derived from Rec5-L and R7f-L were then selectively amplified using the forward primer for viral U3 sequences of the 3' LTR and the reverse primer for the RVP3 sequence. To confirm that the first strand of cDNA that was synthesised with an anti-RVP3 oligo strand contained spliced luciferase-mRNA, PCR was performed using the primer set of f-597 and s2. As a control, the *gapdh*-mRNA and poly (A) tail length of *gapdh*-mRNA were detected in Rec5-L and R7f-L transfected cells. The PCR products were electrophoresed and visualized by ethidium-bromide staining.

gapdh-mRNA (Fig. 2-3).

Following the results showing that 0.3-kb fragment influenced the amount of spliced messages and subsequently the expression of its corresponding luciferase protein, we set out to determine the nuclear-cytoplasmic distribution of the spliced message. NIH3T3 cells transfected with Rec5-L and R7f-L vectors were divided into nuclear and cytoplasmic fractions and total RNA was extracted from each fraction. The separation of nucleus and cytoplasm was confirmed by assaying for the presence of ribosomal RNAs. The mature 18S and 28S ribosomal RNAs were detected predominantly in the cytoplasmic fraction (data not shown). In the cells transfected with Rec5-L, 12% of *luc*-mRNA was detected in the cytoplasmic fraction and 88% was in the nuclear fraction (Fig. 2-4). In the cells transfected with R7f-L, 17% of *luc*-mRNA was detected in the cytoplasmic fraction and 83% was in the nuclear fraction. In both types of cell, *gapdh*-mRNA was predominantly in the cytoplasmic fraction, with 59% (Rec5-L) and 65% (R7f-L) of the *gapdh*-mRNA in the cytoplasm and about 41% (Rec5-L) and 35% (R7f-L) remaining in the nucleus (Fig. 2-4). The distribution of *luc*-mRNA in the nucleus and cytoplasm of the cells with introduced Rec5-L and R7f-L was not significantly different.

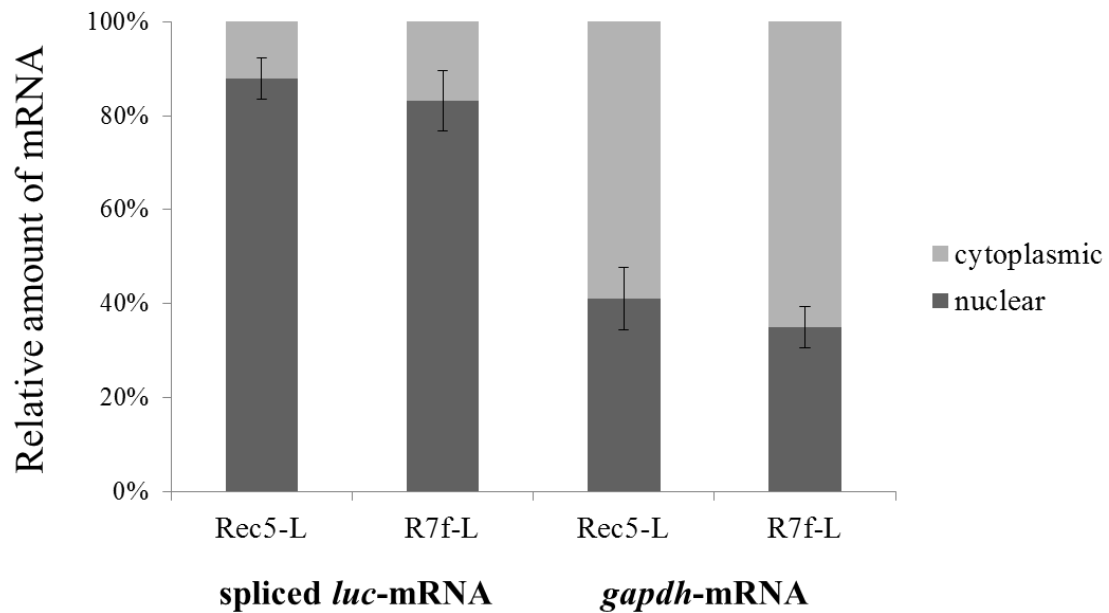


Figure 2-4

Nuclear-cytoplasmic distribution of *luc*-mRNA. Nuclear and cytoplasmic fractions were obtained from NIH3T3 cells transfected with R7f-L and Rec5-L and RNA was extracted from each fraction. The amount of *spliced*-mRNA and *gapdh*-mRNA in each fraction was quantified by real-time RT-PCR. The mean values from 3 independent experiments and the SEM are shown. Statistical comparison was done using the *t* test.

Point mutation analysis

Further investigations were carried out to determine whether any of the nucleotides within the 0.3-kb fragment are key(s) to the observed luciferase expression effects. Using the same luciferase expression vectors, a series of point mutations was incorporated into the R7f-L 0.3-kb fragment, in which the 17 nucleotides that differ between the A8 and 57 sequences were gradually mutated into sequences of 57 from the 5' site. The luciferase activity of these vectors was determined (Fig. 2-5). F1-L, which has its first four nucleotides exchanged for 57 sequences, showed results comparable to those obtained for R7f-L. Interestingly, when further mutations were introduced at the 5th nucleotide in F2-L, the luciferase activity decreased to 67% ($p < 0.001$) compared to F1-L. The luciferase activity of F3-L, in which further mutations were introduced at the 6th and 7th nucleotides, decreased to 50% and was lower than that of F2-L ($p < 0.001$). The luciferase activity of F4-L, in which further mutations were introduced at the 8th nucleotide, was the same as that of F3-L. On the other hand, we constructed the B series vectors in which mutations were incorporated from the 3' site of 0.3-kb fragment. When the 9th to 14th nucleotides were further exchanged for their 57 counterparts, the luciferase activity showed no significant difference compared to R7f-L in B2-L (101%) and B3-L (87%).

After evaluating the results of experiments with the F series vectors, we asked if the 5th, 6th and 7th nucleotides alone could contribute to the regulation of luciferase activity. Towards this end, we constructed: (a) R7f.567m-L, in which only the 5th, 6th and 7th nucleotides contain the 57 sequences and (b) another vector having the exact reverse order, Rec5.567m-L, which has only the 5th, 6th and 7th sequences retained as A8 sequences. The luciferase activity of R7f.567m-L remained at about 95% and could not be brought down to parallel that of Rec5-L, while its exact reverse vector, Rec5.567m-L, had a significantly increased luciferase activity (86%) that was higher than that of Rec5-L ($p < 0.001$).

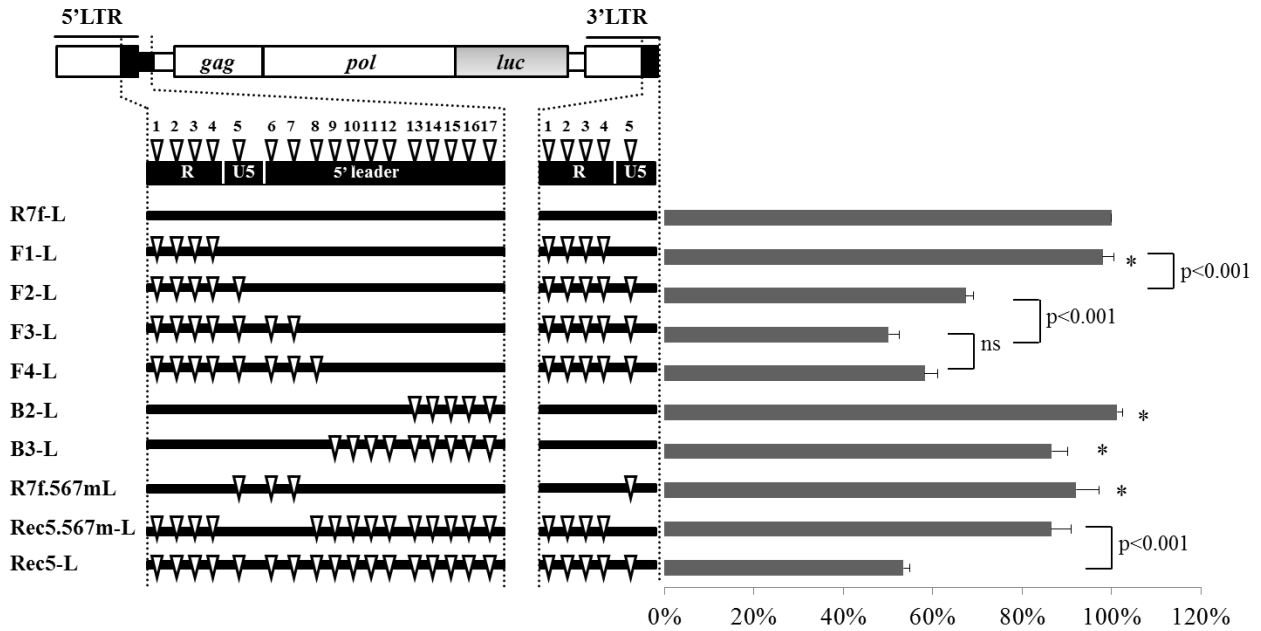


Figure 2-5

Luciferase activity of mutation series vectors. A series of vectors where the sequences from A8 were gradually mutated into 57 sequences were constructed and their luciferase activities were quantified. Mutations from A8 to 57 are indicated by triangles. The mean values from 4-7 independent experiments and the SEM are shown. Statistical comparison was done using the t test. ns: differences were not significant.

*: differences were not significant versus R7f-L.

Secondary structure analysis

To explain how the 1st to 7th nucleotides might be important for *luc*-mRNA expression, we mapped out the secondary structure formed by the sequence containing the 1st to 7th nucleotides of the 0.3-kb fragment of the A8 and 57 sequences. The secondary structure, as shown in Figure 2-6 was predicted using MFOLD software. Appropriate regions were selected where the sequence should be truncated by referring to previous studies that had utilized chemical structural probing, NMR, and a functional analysis of Mo-MLV (D'Souza et al., 2004; D'Souza and Summers, 2004; Mougel et al., 1993). Figure 2-6 illustrates the major functional secondary structures of MLV. At first glance, there is not a striking difference between the two secondary structures generated, despite the 7 nucleotides that differ between the A8 and 57 sequences. The most visible changes actually occur upstream from the polyadenylation signal, where the 1st, 2nd, and 3rd nucleotides are incorporated into a stem structure in the A8 sequence, thereby lengthening the stem structure compared to the 57 sequence. The site with the smallest conformational change contains the 5th, 6th and 7th nucleotides. These three nucleotides reside within a stem-loop structure that protrudes out into the PBS. The possible roles played by these nucleotides are discussed further in the next section.

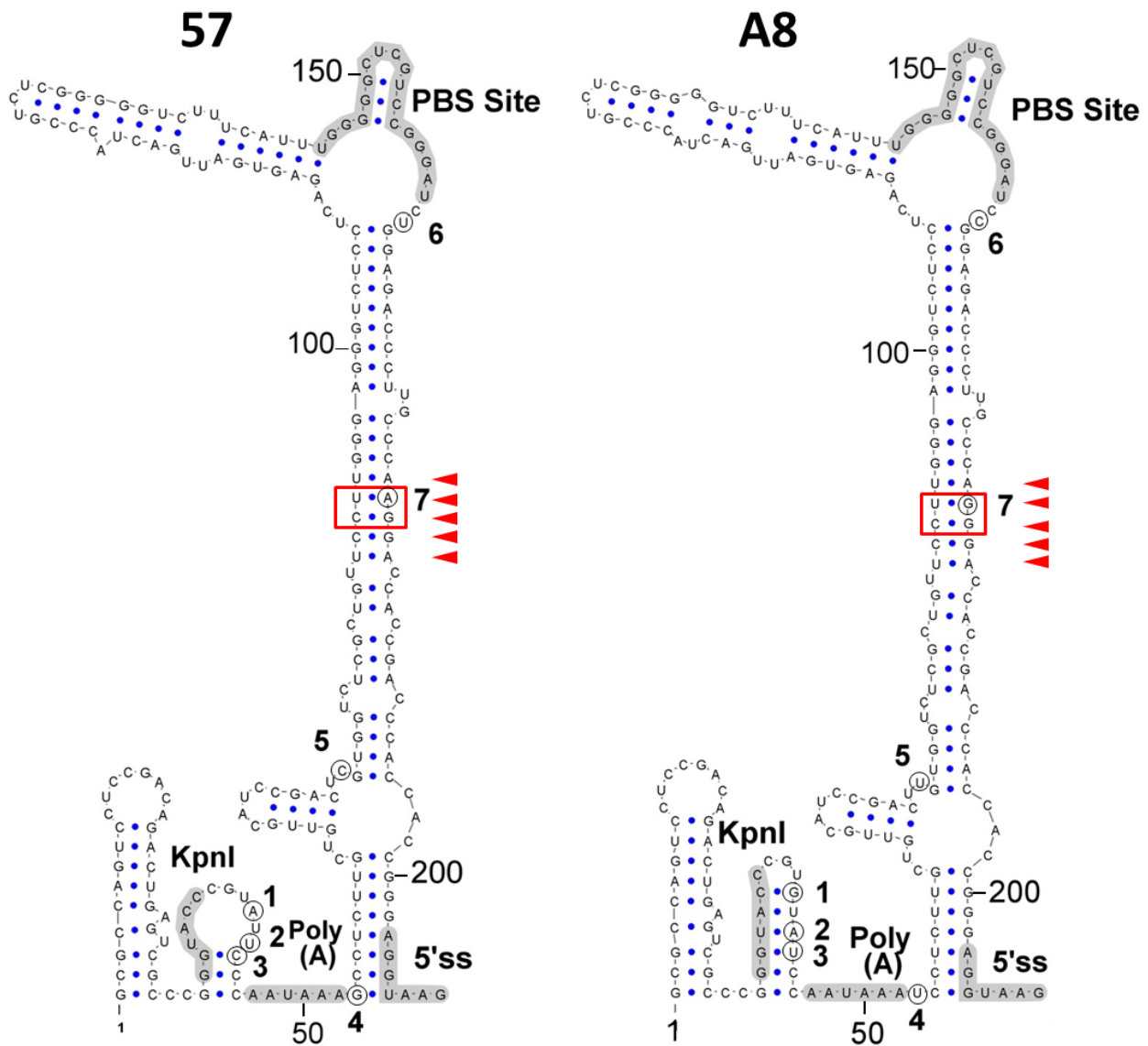


Figure 2-6

Predicted secondary structure of the 0.3-kb fragment of the A8 sequence (accession no. D88386) and the 57 sequence (accession no. X02794). This representation shows the results of an MFOLD simulation and the figure was drawn using VARNA software [(Darty et al., 2009). Nucleotides that differ between A8 and 57 are circles and numbered from 1 to 7. Important regulatory signals are highlighted. PolyA: polyadenylation signal; PBS: primer binding site; 5'ss: 5'splice site; Stem loop A-D: packaging signal of retroviruses. Restriction enzyme site KpnI is shown.

Alignment of the 0.3-kb fragment sequences among gamma retroviruses

Since point mutational analysis indicated the 1st to 7th nucleotides contribute to the luciferase activities of the vectors, we compared the sequences including these nucleotides in gamma retroviruses containing MLVs, Feline leukemia virus (FLV), and Gibbon ape leukemia virus (GALV) (Table 2-1). The 1st guanine (G) nucleotide in A8 was well conserved among these gamma retroviruses except for 57. The 2nd and 3rd nucleotides in A8 were adenine (A) and thymidine (T), respectively, and the 4th, 5th, and 6th nucleotides in 57 were G, cytosine (C), and T, respectively. These nucleotides were relatively conserved among the gamma retroviruses that were analyzed. The 7th guanine nucleotide in A8 was well conserved in not only MLVs but also in FLV and the GALV. Among the sequences analyzed, only the Fr-MLV clone 57 virus had an adenine at the 7th nucleotide.

❖ Discussion

In the present study, to investigate the role of a 0.3-kb KpnI-AatII fragment containing the R-U5-5' leader sequence, recombinant luciferase vectors were constructed by replacing the viral-*env*-gene with the *luc*-gene in proviral sequences to produce R7f-L and Rec5-L (Fig. 2-1). As shown in Fig. 2-2A, R7f-L exhibited about 2 times higher luciferase expression compared to Rec5-L. This result agrees well with experiments that utilized the chimeric viruses R7f and Rec5, in which the Env protein expression level of R7f-infected cells was higher than that of Rec5-infected cells (Takase-Yoden and Watanabe, 2005). Therefore, the experimental system using R7f-L and Rec5-L vectors is useful to analyze the function of the 0.3-kb fragment in Env protein expression. Next, to examine whether the 0.3-kb fragment functions in the 5'LTR-leader sequence and/or in the 3'LTR, we constructed R7fa-L and R7fb-L. R7fa-L contains the 0.3-kb fragment of A8 sequences only at the 5'LTR, and R7fb-L contains the 57 sequences at the 5'LTR but has the A8 sequences of the R-U5 region at the 3'LTR (Fig. 2-1). The results of a luciferase assay showed that R7fa-L mimics the expression level of R7f-L (Fig. 2-2A). R7fb-L, despite having partial A8 sequences at its 3'LTR, had a similarly reduced expression level of Rec5-L. These results suggested that luciferase expression is dependent solely on the 0.3-kb sequences at the 5'LTR-leader sequence rather than the sequences at the 3'LTR.

In the luciferase expression vector system of the present study, luciferase protein is translated from spliced mRNA. When quantified in transfected cells, the amount of spliced *luc*-mRNA in the cells transfected with R7f-L was about 2 times higher than that in the cells transfected with Rec5-L (Fig. 2-2B). Furthermore, the amount of spliced *luc*-mRNA of R7fa-L was equivalent to the amount of spliced *luc*-mRNA of R7f-L, and R7fb-L showed the same amount of spliced *luc*-mRNA as Rec5-L (Fig. 2-2B). The amount of spliced transcripts from the vectors correlated with the luciferase activities (Fig. 2-2A). These results indicated that the 0.3-kb fragment of A8 enhanced luciferase expression levels by increasing the amount of spliced *luc*-mRNA. This raised the

question of how the 0.3-kb fragment of A8 enhanced the amount of spliced *luc*-mRNA. Because the amount of total transcripts, including unspliced mRNA and spliced mRNA, was the same among Rec5-L, R7f-L, R7fa-L, and R7fb-L (Fig. 2-3B), the 0.3-kb fragment seems to not affect the transcriptional step. Other steps in the maturation of transcripts were also investigated, e.g. the poly (A) tail length and the nuclear export of transcripts from vectors. We could not observe any differences between the poly (A) tail length of mRNA in the R7f-L versus the Rec5-L transfected cells (Fig. 2-3). The nuclear-cytoplasmic distribution of spliced *luc*-mRNA was the same for the R7f-L and the Rec5-L transfected cells (Fig. 2-4), indicating that the efficiency of nuclear export of spliced *luc*-mRNA was the same for both R7f-L and Rec5-L. These results suggest that the 0.3-kb fragment contributes to the splicing efficiency of transcripts and that luciferase expression is enhanced by the role of the 0.3-kb fragment of A8 in promoting splicing. As shown in figure 2-3, the poly (A) tail length of viral mRNA was longer than that of *gadh*-mRNA. The reason for this phenomenon is not clear, but release of poly (A) polymerase from viral mRNA might be suppressed. The nuclear-cytoplasmic distribution of mRNA also differs between viral mRNA and *gadh*-mRNA. It is generally known that nuclear export of mRNA is mediated by multiple protein factors that couple steps of nuclear pre-mRNA biogenesis to mRNA transport (Cole and Scarcelli, 2006) therefore, different factors might be recruited in viral mRNA compared to *gadh*-mRNA.

Next, to investigate the roles of nucleotides that differ between A8 and 57 within the 0.3-kb fragment, we gradually mutated the 17 nucleotides that differ between them and tested their respective luciferase activities. Among the vectors investigated, only the F3-L, which carries the 1st to 7th nucleotides of 57 on the background of the A8 sequence, showed decreased luciferase activity that paralleled that of Rec5-L, which has the 57 sequence (Fig. 2-5). Furthermore, R7f.567m-L, which has only the 5th, 6th and 7th sequences retained as 57 sequences, showed luciferase activity that remained at about 95% and could not be brought down to parallel that of Rec5-L. These results suggested that the 1st to 7th nucleotide of the 0.3-kb fragment were important regulators of the

luciferase protein expression level.

To illustrate how the 1st to 7th nucleotides of the 0.3-kb fragment may be functionally important, a secondary structure was drawn for the fragment containing the 1st to 7th nucleotides of the A8 and 57 sequences, as shown in figure 2-6. The 5th, 6th and 7th nucleotides, which mutational analysis had shown were primary contributors to increased luciferase expression, reside within a stem-loop structure that protrudes out into the PBS. It was previously reported that sequences upstream of the 5'ss negatively regulate the splicing of MLV by forming a secondary structure (Kraunus et al., 2006). Kraunus et al. argue that the stem structure plays a role upstream of the 5'ss in determining the accessibility for cellular splice regulators. According to Zychlinski et al., the stem structure or region surrounding the 5'ss regulates the splice donor to be accessed by U1snRNA, thereby regulating MLV splicing (Zychlinski et al., 2009). The stability and integrity of the stem-loop structure containing PBS is important to determine the splicing efficiency: higher stability of the stem-loop structure seems to inhibit splicing more efficiently. Similarly, in HIV type 1, it has been reported that the stable hairpin-structure of RNA containing the major 5'ss suppresses the activity of the 5'ss (Abbink and Berkhout, 2008). Interestingly, as shown in figure 2-6, the 4th to 7th nucleotides take part in the formation of secondary structure around the 5'ss. Because the secondary structure formed by A8 releases free energy of $dG=-72.5\text{kcal/mol}$, while 57 releases $dG=-75.1\text{kcal/mol}$, the stem structure of the 57 sequence is likely more stable than the A8 sequence. This suggests that the stem structure of the 57 sequence inhibits splicing more efficiently than the stem structure of the A8 sequence, resulting in decreased luciferase activity. Kraunus et al. have studied the AGGGA motif in the stem structure, which is a potential binding motif for hnRNPA1, a splice repressor. The results of experiments in which the AGGGA motif was mutated have shown that this sequence contributes to splicing efficiency through altering the secondary structure stability rather than the sequence motif. The AGGGA motif in the A8 sequence is also found around the 7th nucleotide, as shown by arrowheads in figure 2-6. This motif may be demolished by changing the

A8-G sequence at the 7th nucleotide of 57 to adenine, which may decrease the binding of hnRNPA1, the splice repressor; however, contrary to expectations, luciferase expression was decreased. In examining the secondary structure, the base corresponding to the 7th G on the ascending side of the stem is U in the A8 sequence, while the base corresponding to the 7th A on the ascending side of the stem is U in the 57 sequence (Fig. 2-6, boxed motif). Kraunus et al. reported that the higher complementarity of bases facing each other in the boxed motif decreased the splicing efficiency. This suggests that the 7th nucleotide plays an important role in luciferase expression by participating in the splicing step. Alignment of the gamma retroviral 0.3-kb fragment sequences showed that the A8-guanine at the 7th position is conserved among the FLV, GALV, and MLV sequences except for 57, while the A8-thymine and A8-cytosine at the 5th and 6th positions, respectively, are less conserved (Table 2-1). The 7th nucleotide is likely to be important for gene expression of gamma retroviruses, which might explain the different activities of the 0.3-kb fragments of A8 and 57. The roles of the 1st to 4th nucleotides are not yet known, but a change of secondary structure between A8 and 57 has been observed (Fig. 2-6) and this stem loop structure may also contribute to luciferase expression through tertiary interactions with the stem loop structure formed by the sequence containing the 5th to 7th nucleotides.

CONCLUSION

This study has tried to elucidate the molecular mechanisms for the regulation of gene expression by a 0.3-kb fragment containing the R-U5-5' leader sequence of MLV. The 0.3-kb fragment has been determined as an important determinant for inducing spongiosis, in addition to the env gene of A8 as the primary determinant by the studies with chimeras constructed from a neuropathogenic variant of Fr-MLV clone A8 and the non-neuropathogenic Fr-MLV clone 57. The 0.3-kb fragment contains a 17-nucleotide difference between the A8 and 57 sequences. We previously showed that the 0.3-kb fragment influences expression levels of Env protein in both cultured cells and rat brain, but the corresponding molecular mechanisms are not well understood.

First, we carried out kinetic studies using two recombinant viruses, R7f, which contains the 0.3-kb fragment of A8 and the A8-env gene on the background of 57, and Rec5, which contains the A8-env gene on the background of 57. The viral growth curves, amount of total viral-mRNA, and Gag protein was comparable between R7f and Rec5. Env protein expression was in agreement with previous studies showing about 3- to 4-fold higher expression in R7f-infected cell compared to Rec5-infected cells. In concordant to the level of Env protein, amount of spliced-env mRNA was found to be higher in R7f compared to Rec5. These results suggested that the 0.3-kb fragment influenced the expression level of the Env protein by regulating the amount of spliced env-mRNA rather than the amount of total viral mRNA or viral production.

To fully elucidate the role of the 0.3-kb fragment in Env protein expression, we performed analysis using a vector containing the 0.3-kb fragment and a reporter gene. Studies with expression vectors constructed from the full-length proviral genome of Fr-MLV that incorporated the luciferase (luc) gene instead of the env gene found that the vector containing the A8-0.3-kb fragment yielded a larger amount of spliced luc-mRNA and showed higher expression of luciferase when compared to the vector containing the 57-0.3-kb fragment. To examine effects of the 0.3-kb fragment on other

processes of gene expression, the amount of total transcripts from the vectors, the poly (A) tail length of their mRNAs, and the nuclear-cytoplasm distribution of luc-mRNA in transfected cells were also evaluated. The 0.3-kb fragment did not influence transcription efficiency, mRNA polyadenylation or nuclear export of luc-mRNA. Taken together, these data indicate that the 0.3-kb fragment containing the R-U5-5' leader sequence of Fr-MLV influences the level of protein expression from the spliced-mRNA by regulating the splicing efficiency rather than transcription, nuclear export of spliced-mRNA, or poly (A) addition to mRNA.

Furthermore, mutational analyses were carried out to determine the importance of nucleotides that differ between the A8 and 57 sequences within the 0.3-kb fragment. Results from the point mutation analysis indicated that seven nucleotides upstream of the 5'ss were found to be important in regulating the level of protein expression from spliced messages. Secondary structure analysis as well as alignment study of sequences among gamma retroviruses suggested that particularly, three nucleotide within the stem-loop structure affected the stability of the stem structure that has been speculated to limit the recognition of the 5'ss.

Throughout the promoter and the 5' leader sequence of retroviruses, there is an aggregation of cis-elements and structural conformations that regulate many steps within the replication of retroviruses. This study, which demonstrated the involvement of the 0.3-kb fragment containing the R-U5-5' leader sequence in splicing, contributes to one of the myriad examples of the role carried from the non-coding region of retroviruses.

REFERENCES

- Aagaard, L., S. V. Rasmussen, J. G. Mikkelsen, and F. S. Pedersen, 2004, Efficient replication of full-length murine leukemia viruses modified at the dimer initiation site regions: *Virology*, v. 318, p. 360-70.
- Abbink, T. E., and B. Berkhout, 2008, RNA structure modulates splicing efficiency at the human immunodeficiency virus type 1 major splice donor: *J Virol*, v. 82, p. 3090-8.
- Abelson, H. T., and L. S. Rabstein, 1970a, Influence of prednisolone on Moloney leukemogenic virus in BALB-c mice: *Cancer Res*, v. 30, p. 2208-12.
- Abelson, H. T., and L. S. Rabstein, 1970b, Lymphosarcoma: virus-induced thymic-independent disease in mice: *Cancer Res*, v. 30, p. 2213-22.
- Aiyar, A., D. Cobrinik, Z. Ge, H. J. Kung, and J. Leis, 1992, Interaction between retroviral U5 RNA and the T psi C loop of the tRNA(Trp) primer is required for efficient initiation of reverse transcription: *J Virol*, v. 66, p. 2464-72.
- Askovic, S., C. Favara, F. J. McAtee, and J. L. Portis, 2001, Increased expression of MIP-1 alpha and MIP-1 beta mRNAs in the brain correlates spatially and temporally with the spongiform neurodegeneration induced by a murine oncornavirus: *J Virol*, v. 75, p. 2665-74.
- Badorrek, C. S., C. M. Gherghe, and K. M. Weeks, 2006, Structure of an RNA switch that enforces stringent retroviral genomic RNA dimerization: *Proc Natl Acad Sci U S A*, v. 103, p. 13640-5.
- Baltimore, D., 1970, RNA-dependent DNA polymerase in virions of RNA tumour viruses: *Nature*, v. 226, p. 1209-11.
- Bannert, N., and R. Kurth, 2004, Retroelements and the human genome: new perspectives on an old relation: *Proc Natl Acad Sci U S A*, v. 101 Suppl 2, p. 14572-9.
- Bannwarth, S., and A. Gatignol, 2005, HIV-1 TAR RNA: the target of molecular interactions between the virus and its host: *Curr HIV Res*, v. 3, p. 61-71.
- Basyuk, E., S. Boulon, F. Skou Pedersen, E. Bertrand, and S. Vestergaard Rasmussen, 2005, The packaging signal of MLV is an integrated module that mediates intracellular transport of genomic RNAs: *J Mol Biol*, v. 354, p. 330-9.
- Beerens, N., and J. Kjems, 2010, Circularization of the HIV-1 genome facilitates strand transfer during reverse transcription: *RNA*, v. 16, p. 1226-35.
- Berkhout, B., and J. L. van Wamel, 2000, The leader of the HIV-1 RNA genome forms a compactly folded tertiary structure: *RNA*, v. 6, p. 282-95.
- Berkhout, B., N. L. Vastenhouw, B. I. Klasens, and H. Huthoff, 2001, Structural features in the HIV-1 repeat region facilitate strand transfer during reverse transcription: *RNA*, v. 7, p. 1097-114.
- Berlioz, C., and J. L. Darlix, 1995, An internal ribosomal entry mechanism promotes translation of murine leukemia virus gag polyprotein precursors: *J Virol*, v. 69, p. 2214-22.
- Bess, J. W., Jr., R. J. Gorelick, W. J. Bosche, L. E. Henderson, and L. O. Arthur, 1997, Microvesicles are a source of contaminating cellular proteins found in purified HIV-1 preparations: *Virology*, v. 230, p.

- Bishop, J. M., 1991, Molecular themes in oncogenesis: *Cell*, v. 64, p. 235-48.
- Bittner, J. J., 1942, THE MILK-INFLUENCE OF BREAST TUMORS IN MICE: *Science*, v. 95, p. 462-3.
- Bonwetsch, R., S. Croul, M. W. Richardson, C. Lorenzana, L. Del Valle, A. E. Sverstiuk, S. Amini, S. Morgello, K. Khalili, and J. Rappaport, 1999, Role of HIV-1 Tat and CC chemokine MIP-1alpha in the pathogenesis of HIV associated central nervous system disorders: *J Neurovirol*, v. 5, p. 685-94.
- Brooks, B. R., J. Gossage, and R. T. Johnson, 1981, Age-dependent in vitro restriction of mouse neurotropic retrovirus replication in central nervous system-derived cells from susceptible Fv-1nn mice: *Trans Am Neurol Assoc*, v. 106, p. 238-41.
- Cantin, R., J. Diou, D. Belanger, A. M. Tremblay, and C. Gilbert, 2008, Discrimination between exosomes and HIV-1: purification of both vesicles from cell-free supernatants: *J Immunol Methods*, v. 338, p. 21-30.
- Choe, W., G. Stoica, W. Lynn, and P. K. Wong, 1998, Neurodegeneration induced by MoMuLV-ts1 and increased expression of Fas and TNF-alpha in the central nervous system: *Brain Res*, v. 779, p. 1-8.
- Coffin, J. M., S. H. Hughes, and H. E. Varmus, 1997a, *Oncogenesis, Retroviruses*: Cold Spring Harbor (NY), Cold Spring Harbor Laboratory Press.
- Coffin, J. M., S. H. Hughes, and H. E. Varmus, 1997b, *Purification, Composition, and Morphology of Virions, Retroviruses*, Cold Spring Harbor Laboratory Press.
- Coffin, J. M., S. H. Hughes, and H. E. Varmus, 1997c, *Retroviruses*: New York, Cold Spring Harbor Laboratory Press.
- Coffin, J. M., S. H. Hughes, and H. E. Varmus, 1997d, *The Development of Retrovirology as Intellectual History: Retroviruses*.
- Cole, C. N., and J. J. Scarcelli, 2006, Transport of messenger RNA from the nucleus to the cytoplasm: *Curr Opin Cell Biol*, v. 18, p. 299-306.
- Cork, L. C., W. J. Hadlow, T. B. Crawford, J. R. Gorham, and R. C. Piper, 1974, Infectious leukoencephalomyelitis of young goats: *J Infect Dis*, v. 129, p. 134-41.
- Crawford, T. B., D. S. Adams, W. P. Cheevers, and L. C. Cork, 1980, Chronic arthritis in goats caused by a retrovirus: *Science*, v. 207, p. 997-9.
- Czub, M., S. Czub, F. J. McAtee, and J. L. Portis, 1991, Age-dependent resistance to murine retrovirus-induced spongiform neurodegeneration results from central nervous system-specific restriction of virus replication: *J Virol*, v. 65, p. 2539-44.
- D'Souza, V., A. Dey, D. Habib, and M. F. Summers, 2004, NMR structure of the 101-nucleotide core encapsidation signal of the Moloney: *J Mol Biol*, v. 337, p. 427-42.
- D'Souza, V., and M. F. Summers, 2004, Structural basis for packaging the dimeric genome of Moloney murine leukaemia virus: *Nature*, v. 431, p. 586-90.
- Darty, K., A. Denise, and Y. Ponty, 2009, VARNA: Interactive drawing and editing of the RNA secondary structure: *Bioinformatics*, v. 25, p. 1974-5.

- Delgado, E., C. Carrera, P. Nebreda, A. Fernandez-Garcia, M. Pinilla, V. Garcia, L. Perez-Alvarez, and M. M. Thomson, 2012, Identification of new splice sites used for generation of rev transcripts in human immunodeficiency virus type 1 subtype C primary isolates: *PLoS One*, v. 7, p. e30574.
- Derse, D., and J. W. Casey, 1986, Two elements in the bovine leukemia virus long terminal repeat that regulate gene expression: *Science*, v. 231, p. 1437-40.
- DesGroseillers, L., M. Barrette, and P. Jolicoeur, 1984, Physical mapping of the paralysis-inducing determinant of a wild mouse ecotropic neurotropic retrovirus: *J Virol*, v. 52, p. 356-63.
- Dimcheff, D. E., S. Askovic, A. H. Baker, C. Johnson-Fowler, and J. L. Portis, 2003, Endoplasmic reticulum stress is a determinant of retrovirus-induced spongiform neurodegeneration: *J Virol*, v. 77, p. 12617-29.
- Dimcheff, D. E., M. A. Faasse, F. J. McAtee, and J. L. Portis, 2004, Endoplasmic reticulum (ER) stress induced by a neurovirulent mouse retrovirus is associated with prolonged BiP binding and retention of a viral protein in the ER: *J Biol Chem*, v. 279, p. 33782-90.
- Dudley, J. P., J. A. Mertz, L. Rajan, M. Lozano, and D. R. Broussard, 2002, What retroviruses teach us about the involvement of c-Myc in leukemias and lymphomas: *Leukemia*, v. 16, p. 1086-98.
- Durand, S., X. N. Nguyen, J. Turpin, S. Cordeil, N. Nazaret, S. Croze, R. Mahieux, J. Lachuer, C. Legras-Lachuer, and A. Cimarelli, 2012, Tailored HIV-1 vectors for the genetic modification of primary human dendritic cells and monocytes: *J Virol*.
- Déjardin, J., G. Bompard-Maréchal, M. Audit, T. J. Hope, M. Sitbon, and M. Mougél, 2000, A Novel Subgenomic Murine Leukemia Virus RNA Transcript Results from Alternative Splicing: *J Virol*, v. 74, p. 3709-14.
- Ellerman, V., and O. Bang, 1908, Experimentelle Leukämie bei Hühnern.: *Zentralbl Bakteriol Parasitenkd Infektionskr Hyg Abt Orig*, v. 46:595.
- Friend, C., 1957, Cell-free transmission in adult Swiss mice of a disease having the character of a leukemia: *J Exp Med*, v. 105, p. 307-18.
- Gardner, M. B., 1978, Type C viruses of wild mice: characterization and natural history of amphotropic, ecotropic, and xenotropic MuLV: *Curr Top Microbiol Immunol*, v. 79, p. 215-59.
- Gee, A. H., W. Kasprzak, and B. A. Shapiro, 2006, Structural differentiation of the HIV-1 polyA signals: *J Biomol Struct Dyn*, v. 23, p. 417-28.
- Gifford, R., P. Kabat, J. Martin, C. Lynch, and M. Tristem, 2005, Evolution and distribution of class II-related endogenous retroviruses: *J Virol*, v. 79, p. 6478-86.
- Gilboa, E., S. W. Mitra, S. Goff, and D. Baltimore, 1979, A detailed model of reverse transcription and tests of crucial aspects: *Cell*, v. 18, p. 93-100.
- Gluschankof, P., I. Mondor, H. R. Gelderblom, and Q. J. Sattentau, 1997, Cell membrane vesicles are a major contaminant of gradient-enriched human immunodeficiency virus type-1 preparations: *Virology*, v. 230, p. 125-33.
- Gomez-Lucia, E., 2005, The other transmissible spongiform encephalopathies: *Rev Neurosci*, v. 16, p. 159-79.
- Gould, S. J., A. M. Booth, and J. E. Hildreth, 2003, The Trojan exosome hypothesis: *Proc Natl Acad Sci U S A*, v. 100, p. 10592-7.

- Griffiths, D. J., 2001, Endogenous retroviruses in the human genome sequence: *Genome Biol*, v. 2, p. REVIEWS1017.
- Hardy, W. D., Jr., 1982, Immunopathology induced by the feline leukemia virus: *Springer Semin Immunopathol*, v. 5, p. 75-106.
- Harvey, J. J., 1964, AN UNIDENTIFIED VIRUS WHICH CAUSES THE RAPID PRODUCTION OF TUMOURS IN MICE: *Nature*, v. 204, p. 1104-5.
- Hauber, J., and B. R. Cullen, 1988, Mutational analysis of the trans-activation-responsive region of the human immunodeficiency virus type I long terminal repeat: *J Virol*, v. 62, p. 673-9.
- Herniou, E., J. Martin, K. Miller, J. Cook, M. Wilkinson, and M. Tristem, 1998, Retroviral diversity and distribution in vertebrates: *J Virol*, v. 72, p. 5955-66.
- Houzet, L., J. C. Paillart, F. Smagulova, S. Maurel, Z. Morichaud, R. Marquet, and M. Mougel, 2007, HIV controls the selective packaging of genomic, spliced viral and cellular RNAs into virions through different mechanisms: *Nucleic Acids Res*, v. 35, p. 2695-704.
- Ikeda, T., S. Takase-Yoden, and R. Watanabe, 1995, Characterization of monoclonal antibodies recognizing neurotropic Friend murine leukemia virus: *Virus Res*, v. 38, p. 297-304.
- Izquierdo-Useros, N., M. Naranjo-Gomez, J. Archer, S. C. Hatch, I. Erkizia, J. Blanco, F. E. Borrás, M. C. Puertas, J. H. Connor, M. T. Fernandez-Figueras, L. Moore, B. Clotet, S. Gummuluru, and J. Martinez-Picado, 2009, Capture and transfer of HIV-1 particles by mature dendritic cells converges with the exosome-dissemination pathway: *Blood*, v. 113, p. 2732-41.
- Izquierdo-Useros, N., M. Naranjo-Gomez, I. Erkizia, M. C. Puertas, F. E. Borrás, J. Blanco, and J. Martinez-Picado, 2010, HIV and mature dendritic cells: Trojan exosomes riding the Trojan horse?: *PLoS Pathog*, v. 6, p. e1000740.
- Jinno-Oue, A., S. G. Wilt, C. Hanson, N. V. Dugger, P. M. Hoffman, M. Masuda, and S. K. Ruscetti, 2003, Expression of inducible nitric oxide synthase and elevation of tyrosine nitration of a 32-kilodalton cellular protein in brain capillary endothelial cells from rats infected with a neuropathogenic murine leukemia virus: *J Virol*, v. 77, p. 5145-51.
- Jolicoeur, P., C. Hu, T. W. Mak, J. C. Martinou, and D. G. Kay, 2003, Protection against murine leukemia virus-induced spongiform myeloencephalopathy in mice overexpressing Bcl-2 but not in mice deficient for interleukin-6, inducible nitric oxide synthetase, ICE, Fas, Fas ligand, or TNF-R1 genes: *J Virol*, v. 77, p. 13161-70.
- Jones, K. A., P. A. Luciw, and N. Duchange, 1988, Structural arrangements of transcription control domains within the 5'-untranslated leader regions of the HIV-1 and HIV-2 promoters: *Genes Dev*, v. 2, p. 1101-14.
- Kappes, J. C., and X. Wu, 2001, Safety considerations in vector development: *Somat Cell Mol Genet*, v. 26, p. 147-58.
- Kay, M. A., 2011, State-of-the-art gene-based therapies: the road ahead: *Nature Reviews Genetics*, v. 12, p. 316-328.
- Kim, H. T., K. Waters, G. Stoica, W. Qiang, N. Liu, V. L. Scofield, and P. K. Wong, 2004, Activation of endoplasmic reticulum stress signaling pathway is associated with neuronal degeneration in MoMuLV-ts1-induced spongiform encephalomyelopathy: *Lab Invest*, v. 84, p. 816-27.
- King, A. M., E. Lefkowitz, M. J. Adams, and E. B. Carstens, eds., 2012, *Virus taxonomy: classification and nomenclature of viruses: Ninth Report of the International Committee on Taxonomy of*

Viruses: San Diego, Elsevier Academic Press.

- Kirsten, W. H., and L. A. Mayer, 1967, Morphologic responses to a murine erythroblastosis virus: *J Natl Cancer Inst*, v. 39, p. 311-35.
- Kiss-Toth, E., and I. Unk, 1994, A downstream regulatory element activates the bovine leukemia virus promoter: *Biochem Biophys Res Commun*, v. 202, p. 1553-61.
- Kraunus, J., D. Zychlinski, T. Heise, M. Galla, J. Bohne, and C. Baum, 2006, Murine leukemia virus regulates alternative splicing through sequences upstream of the 5' splice site: *Journal of Biological Chemistry*, v. 281, p. 37381-37390.
- Kresina, T. F., 2002, Chapter 4. Vectors in Gene Therapy, *in* K. P. Ponder, ed., *An Introduction to Molecular Medicine and Gene Therapy*: New York, USA., John Wiley & Sons, Inc.,.
- Kung, H. J., C. Boerkoel, and T. H. Carter, 1991, Retroviral mutagenesis of cellular oncogenes: a review with insights into the mechanisms of insertional activation: *Curr Top Microbiol Immunol*, v. 171, p. 1-25.
- Li, W. H., Z. Gu, H. Wang, and A. Nekrutenko, 2001, Evolutionary analyses of the human genome: *Nature*, v. 409, p. 847-9.
- Lund, A. H., J. G. Mikkelsen, J. Schmidt, M. Duch, and F. S. Pedersen, 1999, The kissing-loop motif is a preferred site of 5' leader recombination during replication of SL3-3 murine leukemia viruses in mice: *J Virol*, v. 73, p. 9614-8.
- Lynch, W. P., E. Y. Snyder, L. Qualtiere, J. L. Portis, and A. H. Sharpe, 1996, Late virus replication events in microglia are required for neurovirulent retrovirus-induced spongiform neurodegeneration: evidence from neural progenitor-derived chimeric mouse brains: *J Virol*, v. 70, p. 8896-907.
- Maeda, N., H. Fan, and Y. Yoshikai, 2008, Oncogenesis by retroviruses: old and new paradigms: *Rev Med Virol*, v. 18, p. 387-405.
- Masuda, M., P. M. Hoffman, and S. K. Ruscetti, 1993, Viral determinants that control the neuropathogenicity of PVC-211 murine leukemia virus in vivo determine brain capillary endothelial cell tropism of the virus in vitro: *J Virol*, v. 67, p. 4580-7.
- Masuda, M., M. P. Remington, P. M. Hoffman, and S. K. Ruscetti, 1992, Molecular characterization of a neuropathogenic and nonerythroleukemogenic variant of Friend murine leukemia virus PVC-211: *J Virol*, v. 66, p. 2798-806.
- Maurel, S., L. Houzet, E. L. Garcia, A. Telesnitsky, and M. Mougel, 2007, Characterization of a natural heterodimer between MLV genomic RNA and the SD' retroelement generated by alternative splicing: *RNA*, v. 13, p. 2266-76.
- Miller, J. T., Z. Ge, S. Morris, K. Das, and J. Leis, 1997, Multiple biological roles associated with the Rous sarcoma virus 5' untranslated RNA U5-IR stem and loop: *J Virol*, v. 71, p. 7648-56.
- Miller, R. J., and O. Meucci, 1999, AIDS and the brain: is there a chemokine connection?: *Trends Neurosci*, v. 22, p. 471-9.
- Mittelbrunn, M., and F. Sanchez-Madrid, 2012, Intercellular communication: diverse structures for exchange of genetic information: *Nat Rev Mol Cell Biol*, v. 13, p. 328-35.
- Miyazaki, Y., R. N. Irobalieva, B. S. Tolbert, A. Smalls-Mantey, K. Iyalla, K. Loeliger, V. D'Souza, H. Khant, M. F. Schmid, E. L. Garcia, A. Telesnitsky, W. Chiu, and M. F. Summers, 2010, Structure

of a conserved retroviral RNA packaging element by NMR spectroscopy and cryo-electron tomography: *J Mol Biol*, v. 404, p. 751-72.

- Moloney, J. B., 1960, Biological studies on a lymphoid-leukemia virus extracted from sarcoma 37. I. Origin and introductory investigations: *J Natl Cancer Inst*, v. 24, p. 933-51.
- Montagne, J., and P. Jalinot, 1995, Characterization of a transcriptional attenuator within the 5' R region of the human T cell leukemia virus type 1: *AIDS Res Hum Retroviruses*, v. 11, p. 1123-9.
- Morris, S., and J. Leis, 1999, Changes in Rous sarcoma virus RNA secondary structure near the primer binding site upon tRNA Trp primer annealing: *J Virol*, v. 73, p. 6307-18.
- Mougel, M., N. Tounekti, J. L. Darlix, J. Paoletti, B. Ehresmann, and C. Ehresmann, 1993, Conformational analysis of the 5' leader and the gag initiation site of Mo-MuLV RNA and allosteric transitions induced by dimerization: *Nucleic Acids Res*, v. 21, p. 4677-84.
- Muriaux, D., and A. Rein, 2003, Encapsidation and transduction of cellular genes by retroviruses: *Front Biosci*, v. 8, p. d135-42.
- Nagra, R. M., P. G. Burrola, and C. A. Wiley, 1992, Development of spongiform encephalopathy in retroviral infected mice: *Lab Invest*, v. 66, p. 292-302.
- Nagra, R. M., M. P. Heyes, and C. A. Wiley, 1994, Viral load and its relationship to quinolinic acid, TNF alpha, and IL-6 levels in the CNS of retroviral infected mice: *Mol Chem Neuropathol*, v. 22, p. 143-60.
- Narayanan, A., S. Iordanskiy, R. Das, R. Van Duyne, S. Santos, E. Jaworski, I. Guendel, G. Sampey, E. Gerhart, M. Iglesias-Ussel, A. Popratiloff, R. Hakami, K. Kehn-Hall, M. Young, C. Subra, C. Gilbert, C. Bailey, F. Romerio, and F. Kashanchi, 2013, Exosomes derived from HIV-1 infected cells contain TAR RNA: *J Biol Chem*.
- Nguyen, D. G., A. Booth, S. J. Gould, and J. E. Hildreth, 2003, Evidence that HIV budding in primary macrophages occurs through the exosome release pathway: *J Biol Chem*, v. 278, p. 52347-54.
- Ohtani, K., M. Nakamura, S. Saito, T. Noda, Y. Ito, K. Sugamura, and Y. Hinuma, 1987, Identification of two distinct elements in the long terminal repeat of HTLV-I responsible for maximum gene expression: *Embo J*, v. 6, p. 389-95.
- Onafuwa-Nuga, A. A., A. Telesnitsky, and S. R. King, 2006, 7SL RNA, but not the 54-kd signal recognition particle protein, is an abundant component of both infectious HIV-1 and minimal virus-like particles: *Rna*, v. 12, p. 542-6.
- Ooms, M., T. E. Abbink, C. Pham, and B. Berkhout, 2007, Circularization of the HIV-1 RNA genome: *Nucleic Acids Res*, v. 35, p. 5253-61.
- Paquette, Y., Z. Hanna, P. Savard, R. Brousseau, Y. Robitaille, and P. Jolicoeur, 1989, Retrovirus-induced murine motor neuron disease: mapping the determinant of spongiform degeneration within the envelope gene: *Proc Natl Acad Sci U S A*, v. 86, p. 3896-900.
- Peterson, K. E., S. J. Robertson, J. L. Portis, and B. Chesebro, 2001, Differences in cytokine and chemokine responses during neurological disease induced by polytropic murine retroviruses Map to separate regions of the viral envelope gene: *J Virol*, v. 75, p. 2848-56.
- Peyton., R., 1911, A sarcoma of the fowl transmissible by an agent separable from the tumor cells.: *J. Exp. Med.*, v. 13.
- Pierce, J., B. E. Fee, M. G. Toohey, and D. O. Peterson, 1993, A mouse mammary tumor virus promoter

element near the transcription initiation site: *J Virol*, v. 67, p. 415-24.

- Portis, J. L., P. Askovich, J. Austin, Y. Gutierrez-Cotto, and F. J. McAtee, 2009, The degree of folding instability of the envelope protein of a neurovirulent murine retrovirus correlates with the severity of the neurological disease: *J Virol*, v. 83, p. 6079-86.
- Portis, J. L., S. Czub, C. F. Garon, and F. J. McAtee, 1990, Neurodegenerative disease induced by the wild mouse ecotropic retrovirus is markedly accelerated by long terminal repeat and gag-pol sequences from nondefective Friend murine leukemia virus: *J Virol*, v. 64, p. 1648-56.
- Prats, A. C., C. Roy, P. A. Wang, M. Erard, V. Housset, C. Gabus, C. Paoletti, and J. L. Darlix, 1990, cis elements and trans-acting factors involved in dimer formation of murine leukemia virus RNA: *J Virol*, v. 64, p. 774-83.
- Qiang, W., J. M. Cahill, J. Liu, X. Kuang, N. Liu, V. L. Scofield, J. R. Voorhees, A. J. Reid, M. Yan, W. S. Lynn, and P. K. Wong, 2004, Activation of transcription factor Nrf-2 and its downstream targets in response to moloney murine leukemia virus ts1-induced thiol depletion and oxidative stress in astrocytes: *J Virol*, v. 78, p. 11926-38.
- Qiang, W., X. Kuang, J. Liu, N. Liu, V. L. Scofield, A. J. Reid, Y. Jiang, G. Stoica, W. S. Lynn, and P. K. Wong, 2006, Astrocytes survive chronic infection and cytopathic effects of the ts1 mutant of the retrovirus Moloney murine leukemia virus by upregulation of antioxidant defenses: *J Virol*, v. 80, p. 3273-84.
- Rauscher, F. J., 1962, A virus-induced disease of mice characterized by erythrocytopoiesis and lymphoid leukemia: *J Natl Cancer Inst*, v. 29, p. 515-43.
- Ridgway, A. A., H. J. Kung, and D. J. Fujita, 1989, Transient expression analysis of the reticuloendotheliosis virus long terminal repeat element: *Nucleic Acids Res*, v. 17, p. 3199-215.
- Sambrook, J., Fritsch, E.F., and Maniatis T., 1989, *Molecular cloning: a laboratory manual*, v. 2nd: New York, Cold Spring Harbor Laboratory.
- Seelamgari, A., A. Maddukuri, R. Berro, C. de la Fuente, K. Kehn, L. Deng, S. Dadgar, M. E. Bottazzi, E. Ghedin, A. Pumfery, and F. Kashanchi, 2004, Role of viral regulatory and accessory proteins in HIV-1 replication: *Front Biosci*, v. 9, p. 2388-413.
- Segura, M. M., A. Garnier, M. R. Di Falco, G. Whissell, A. Meneses-Acosta, N. Arcand, and A. Kamen, 2008, Identification of host proteins associated with retroviral vector particles by proteomic analysis of highly purified vector preparations: *J Virol*, v. 82, p. 1107-17.
- Sinibaldi-Vallebona, P., P. Lavia, E. Garaci, and C. Spadafora, 2006, A role for endogenous reverse transcriptase in tumorigenesis and as a target in differentiating cancer therapy: *Genes Chromosomes Cancer*, v. 45, p. 1-10.
- Smagulova, F., S. Maurel, Z. Morichaud, C. Devaux, M. Mougel, and L. Houzet, 2005, The highly structured encapsidation signal of MuLV RNA is involved in the nuclear export of its unspliced RNA: *J Mol Biol*, v. 354, p. 1118-28.
- Spadafora, C., 2004, Endogenous reverse transcriptase: a mediator of cell proliferation and differentiation: *Cytogenet Genome Res*, v. 105, p. 346-50.
- Spadafora, C., 2008, A reverse transcriptase-dependent mechanism plays central roles in fundamental biological processes: *Syst Biol Reprod Med*, v. 54, p. 11-21.
- Suerth, J. D., T. Maetzig, M. H. Brugman, N. Heinz, J. U. Appelt, K. B. Kaufmann, M. Schmidt, M. Grez, U. Modlich, C. Baum, and A. Schambach, 2012a, Alpharetroviral self-inactivating vectors:

- long-term transgene expression in murine hematopoietic cells and low genotoxicity: *Mol Ther*, v. 20, p. 1022-32.
- Suerth, J. D., A. Schambach, and C. Baum, 2012b, Genetic modification of lymphocytes by retrovirus-based vectors: *Curr Opin Immunol*.
- Szurek, P. F., E. Floyd, P. H. Yuen, and P. K. Wong, 1990a, Site-directed mutagenesis of the codon for Ile-25 in gPr80env alters the neurovirulence of ts1, a mutant of Moloney murine leukemia virus TB: *J Virol*, v. 64, p. 5241-9.
- Szurek, P. F., P. H. Yuen, J. K. Ball, and P. K. Wong, 1990b, A Val-25-to-Ile substitution in the envelope precursor polyprotein, gPr80env, is responsible for the temperature sensitivity, inefficient processing of gPr80env, and neurovirulence of ts1, a mutant of Moloney murine leukemia virus TB: *J Virol*, v. 64, p. 467-75.
- Szurek, P. F., P. H. Yuen, R. Jerzy, and P. K. Wong, 1988, Identification of point mutations in the envelope gene of Moloney murine leukemia virus TB temperature-sensitive paralytogenic mutant ts1: molecular determinants for neurovirulence: *J Virol*, v. 62, p. 357-60.
- Takase-Yoden, S., M. Wada, and R. Watanabe, 2006, A viral non-coding region determining neuropathogenicity of murine leukemia virus: *Microbiol Immunol*, v. 50, p. 197-201.
- Takase-Yoden, S., and R. Watanabe, 1997, Unique sequence and lesional tropism of a new variant of neuropathogenic Friend murine leukemia virus: *Virology*, v. 233, p. 411-22.
- Takase-Yoden, S., and R. Watanabe, 2005, A 0.3-kb fragment containing the R-U5-5' leader sequence is essential for the induction of spongiform neurodegeneration by A8 murine leukemia virus: *Virology*, v. 336, p. 1-10.
- Temin, H. M., and S. Mizutani, 1970, RNA-dependent DNA polymerase in virions of Rous sarcoma virus: *Nature*, v. 226, p. 1211-3.
- They, C., 2011, Exosomes: secreted vesicles and intercellular communications: *F1000 Biol Rep*, v. 3, p. 15.
- Troxler, D. H., J. K. Boyars, W. P. Parks, and E. M. Scolnick, 1977a, Friend strain of spleen focus-forming virus: a recombinant between mouse type C ecotropic viral sequences and sequences related to xenotropic virus: *J Virol*, v. 22, p. 361-72.
- Troxler, D. H., W. P. Parks, W. C. Vass, and E. M. Scolnick, 1977b, Isolation of a fibroblast nonproducer cell line containing the Friend strain of the spleen focus-forming virus: *Virology*, v. 76, p. 602-15.
- Trubetskoy, A. M., S. A. Okenquist, and J. Lenz, 1999, R region sequences in the long terminal repeat of a murine retrovirus specifically increase expression of unspliced RNAs: *J Virol*, v. 73, p. 3477-83.
- Uchiyama T, Y. J., Sagawa K, Takatsuki K, Uchino H., 1977, Adult T-cell leukemia: clinical and hematologic features of 16 cases.: *Blood*, v. 50, p. 481-92.
- Vagner, S., A. Waysbort, M. Marena, M. C. Gensac, F. Amalric, and A. C. Prats, 1995, Alternative translation initiation of the Moloney murine leukemia virus mRNA controlled by internal ribosome entry involving the p57/PTB splicing factor: *J Biol Chem*, v. 270, p. 20376-83.
- van Kooyk, Y., and T. B. Geijtenbeek, 2003, DC-SIGN: escape mechanism for pathogens: *Nat Rev Immunol*, v. 3, p. 697-709.
- Vlassov, A. V., S. Magdaleno, R. Setterquist, and R. Conrad, 2012, Exosomes: current knowledge of their composition, biological functions, and diagnostic and therapeutic potentials: *Biochim Biophys*

Acta, v. 1820, p. 940-8.

- Vogt, P. K., 2012, Retroviral oncogenes: a historical primer: *Nat Rev Cancer*, v. 12, p. 639-48.
- Watanabe, R., and S. Takase-Yoden, 2006, Neuropathology induced by infection with Friend murine leukemia viral clone A8-V depends upon the level of viral antigen expression: *Neuropathology*, v. 26, p. 188-95.
- Weiss, R. A., 1996, Retrovirus classification and cell interactions: *J Antimicrob Chemother*, v. 37 Suppl B, p. 1-11.
- Wilson, C. A., and K. Cichutek, 2009, The US and EU regulatory perspectives on the clinical use of hematopoietic stem/progenitor cells genetically modified ex vivo by retroviral vectors: *Methods Mol Biol*, v. 506, p. 477-88.
- Wilt, S. G., N. V. Dugger, N. D. Hitt, and P. M. Hoffman, 2000, Evidence for oxidative damage in a murine leukemia virus-induced neurodegeneration: *J Neurosci Res*, v. 62, p. 440-50.
- Xiong, Y., and T. H. Eickbush, 1990, Origin and evolution of retroelements based upon their reverse transcriptase sequences: *Embo j*, v. 9, p. 3353-62.
- Yamamoto, N., and S. Takase-Yoden, 2009, Friend murine leukemia virus A8 regulates Env protein expression through an intron sequence: *Virology*, v. 385, p. 115-25.
- Yuen, P. H., E. Tzeng, C. Knupp, and P. K. Wong, 1986, The neurovirulent determinants of ts1, a paralytogenic mutant of Moloney murine leukemia virus TB, are localized in at least two functionally distinct regions of the genome: *J Virol*, v. 59, p. 59-65.
- Zachary, J. F., T. V. Baszler, R. A. French, and K. W. Kelley, 1997, Mouse Moloney leukemia virus infects microglia but not neurons even though it induces motor neuron disease: *Mol Psychiatry*, v. 2, p. 104-6.
- Zychlinski, D., S. Erkelenz, V. Melhorn, C. Baum, H. Schaal, and J. Bohne, 2009, Limited complementarity between U1 snRNA and a retroviral 5' splice site permits its attenuation via RNA secondary structure: *Nucleic Acids Research*, v. 37, p. 7429-7440.

ACKNOWLEDGEMENT

I am most deeply indebted for this opportunity to be able to study and learn under the guidance of Prof. Sayaka Takase-Yoden. Your patience and encouragements have really helped me to persevere and be able to bring my work to a fruitful completion. Most importantly, your interactions with us have inspired me with the great educator spirit in you in treasuring each student.

My sincere appreciation also goes to my co-supervisors, Prof. Yuri Aoyama and Prof. Shoko Nishihara, for the intense and rewarding discussions that serve as great learning opportunities. Many appreciations also goes to all teachers in the department whom I have had the privilege to seek your advices. Though rarely seen and working behind the scenes, to all the office staffs of our department, your efforts have made all academic developments possible.

To my labmates who supported me throughout these years, no words could express my gratitude to your kindness and warmth always. I have learnt that a laboratory can only be sustained with a team's effort and trust for each other. I am happy to say that at the hardest time of my research, it was because of knowing that I am being sustained by everyone's daily effort that helped me to carry on. I truly hope that our friendships that have been built will continue into the future.

“Education deals with the essence of what it means to be human. No undertaking is more valuable, more sacred.” With the spirit of our university's founder, Daisaku Ikeda who genuinely regards education as a struggle to foster people whom will treasure another human being, it is my greatest pride that above anything else, if these years as a PhD candidate has thought me anything is to live my life with gratitude to humanity.

Lastly, to my mum, fiancée, everybody in the family, and my eternal friends (you all know who you are), THANK YOU FOR BELIEVING IN ME, LOVE YOU ALL!!